Journal of Mathematical Biology (2023) 87:29
https://doi.org/10.1007/s00285-023-01964-y

Mathematical Biology

# A hierarchical intervention scheme based on epidemic severity in a community network

Runzi He[1] · Xiaofeng Luo[1] · Joshua Kiddy K. Asamoah[3] · Yongxin Zhang[1] · Yihong Li[1] · Zhen Jin[2] · Gui-Quan Sun[1,2]

Received: 30 August 2022 / Revised: 1 June 2023 / Accepted: 5 July 2023


**Abstract**

As there are no targeted medicines or vaccines for newly emerging infectious diseases, isolation among communities (villages, cities, or countries) is one of the most effective intervention measures. As such, the number of intercommunity edges (*NIE*) becomes one of the most important factor in isolating a place since it is closely related to normal life. Unfortunately, how *NIE* affects epidemic spread is still poorly understood. In this paper, we quantitatively analyzed the impact of *NIE* on infectious disease transmission by establishing a four-dimensional *SIR* edge-based compartmental model with two communities. The basic reproduction number $R_0(\langle l \rangle)$ is explicitly obtained subject to *NIE* $\langle l \rangle$. Furthermore, according to $R_0(0)$ with zero *NIE*, epidemics spread could be classified into two cases. When $R_0(0) > 1$ for the case 2, epidemics occur with at least one of the reproduction numbers within communities greater than one, and otherwise when $R_0(0) < 1$ for case 1, both reproduction numbers within communities are less than one. Remarkably, in case 1, whether epidemics break out strongly depends on intercommunity edges. Then, the outbreak threshold in regard to *NIE* is also explicitly obtained, below which epidemics vanish, and otherwise break out. The above two cases form a severity-based hierarchical intervention scheme for epidemics. It is then applied to the SARS outbreak in Singapore, verifying the validity of our scheme. In addition, the final size of the system is gained by demonstrating the existence of positive equilibrium in a four-dimensional coupled system. Theoretical results are also validated through numerical simulation in networks with the Pois-

✉ Xiaofeng Luo
luoxiaofeng@nuc.edu.cn

✉ Gui-Quan Sun
gquansun@126.com

1 Department of Mathematics, North University of China, Shanxi, Taiyuan 030051, China

2 Complex Systems Research Center, Shanxi University, Shanxi, Taiyuan 030006, China

3 Department of Mathematics, Kwame Nkrumah University of Science and Technology, Kumasi, Ghana

Published online: 15 July 2023

son and Power law distributions, respectively. Our results provide a new insight into controlling epidemics.

**Keywords** Community · Threshold of intercommunity edges · Networks · Basic reproduction number · The final size

**Mathematics Subject Classification** 05C28 · 92D25

## 1 Introduction

From ancient times, epidemics have been threatening the stability of human societies (Hammarlund et al. 2003; Halloran et al. 2002; Keeling and Gilligan 2000; Haynes et al. 1996; Lu et al. 2008; Horby 2013; Guo et al. 2015). In particular, recently, the newly emerging infectious diseases, such as Zika (Kostyuchenko et al. 2016; Larocca et al. 2016), Ebola (Pandey et al. 2014; Butler 2014), COVID-19 (Bavel et al. 2020; Cao 2020; Ma et al. 2022) have been aggravating human health. Since there is no targeted medicine and vaccine against these diseases at the beginning, isolation among communities (villages, cities, or countries) is one of the most effective intervention measures (Luo and Jin 2020; Zuzek et al. 2015; Mt et al. 2020). However, isolation would affect normal life. When a community is completely isolated, all relationships between this community and the outside world are cut off. Such isolation will lead to huge impact on the locals. In contrast, incomplete isolation only cuts off some relationships for this community, and partial relationships with outside keep. It may reduce the impact but epidemics may still break out there (Luo and Jin 2020). Therefore, it is desirable to determine how many connections should be cut off making epidemics vanish and impact minimum when an epidemic comes. To the best of our knowledge, this problem is poorly understood so far.

Network epidemic modelling with the consideration of control measures is one of the powerful tools in studying the effects of control intervention on epidemic spread (Luo and Jin 2020; Mt et al. 2020; Bajiya et al. 2021; Peng et al. 2020; Lloyd-Smith et al. 2009; Feng et al. 2022; Chowdhury et al. 2020; Boily et al. 2002; Fraser et al. 2004; Momoh and Fügenschuh 2018; Singh et al. 2018; Arino et al. 2021; Yuan et al. 2022; Nowzari et al. 2016). Currently, such modelling is mainly based on network topology control (Luo and Jin 2020; Feng et al. 2022; Kang et al. 2017; de Jesus Esquivel-Gómez and Barajas-Ramírez 2019; Strona and Castellano 2018), immunization control (Pastor-Satorras and Vespignani 2002; Madar et al. 2004; Fu et al. 2008) and optimal control (Forster and Gilligan 2007; Yan and Zou 2008; Iacoviello and Stasio 2013; Buonomo et al. 2014; Kandhway and Kuri 2014a, b; Chen and Sun 2014a, b). The first class of control is unique for network epidemic models and the later two classes of control are also general in epidemic models without network. At the aspect of network topology control, isolation could change the topological structure to affect the spread of infectious diseases. Research on network topological parameters will bring great benefits to analyze the spread law of infectious diseases (Luo and Jin 2020; Feng et al. 2022; Jin et al. 2011). Isolating nodes with high degrees at different time not only inhibits the epidemics spread but also may prevent larger outbreak (Luo

and Jin 2020). The clustering coefficient is increased by isolation and quarantine to reduce the final size of COVID-19 (Feng et al. 2022). Population with targeted degrees has been isolated to effectively contain the infectious diseases with the minimum costs (Jin et al. 2011). Such research is superior to network epidemic modelling only isolating infected people (Kang et al. 2017) or protecting the susceptible (self-production of susceptible) (de Jesus Esquivel-Gómez and Barajas-Ramírez 2019) not considering variation of network structure. Impacts of community structure on epidemics spread are also not neglected (Jin et al. 2001; Liu and Hu 2005; Rowthorn et al. 2009; Salathé and Jones 2010; Huang and Li 2007; Xu et al. 2019; Clara et al. 2016), which would be introduced in detailed in the next paragraph. For immunization control and optimal control, in the past two decades, various immunization measures have been introduced into network epidemic models to study their effects on the outbreak of infectious diseases, such as targeted immunization (Pastor-Satorras and Vespignani 2002), acquaintance immunization (Madar et al. 2004) and local immunization (Fu et al. 2008). For the limited medical resources, an optimal strategy is to utilize bounded time-varying control to balance the control cost and control goal. The optimal control in network epidemic models were mainly focused on homogeneous contact networks of low-dimension systems (Forster and Gilligan 2007; Yan and Zou 2008; Iacoviello and Stasio 2013; Buonomo et al. 2014; Kandhway and Kuri 2014a, b; Koch et al. 2013; Li et al. 2018) and heterogeneous networks (Chen and Sun 2014a, b).

Achievements in research of impacts of community structure on epidemics spread have already had a lot (Jin et al. 2001; Liu and Hu 2005; Rowthorn et al. 2009; Salathé and Jones 2010). Huang and Li (2007) and Xu et al. (2019) studied the influence of network structure on infectious diseases in scale-free networks with community structure. The former found that the network with strong community structure contributes to reduce the risk of infectious diseases in the network. The latter indicated that the individual behaviour of different communities may tend to cluster synchronization and obtained the epidemic threshold of the model. Clara et al. (2016) indicated that community structure can not only promote the diffusion process but also inhibit the diffusion process. Koch et al. (2013) and Li et al. (2018) directly showed that random removal of edges and reduction of the ratio of external edges within and between communities can reduce the basic reproduction number and the final size. Concerning the dependence of the basic reproduction number on the average degree between communities, Arino et al. (2019) obtained the threshold number of source patches for population persistence by considering the metapopulation model.

It has been indicated that the structure of community network has great influence on the spread of infectious diseases. As described in the first paragraph, for a newly emerging infectious diseases, it is of great importance for decision makers to know the number of connections that could be cut off among communities making epidemics vanish and impact minimum when an epidemic comes. The basic reproduction number is a key index of judging whether epidemics break out or not. It enlightens us to apply the network epidemic modelling to quantitatively study the influence of the number of intercommunity edges (*NIE*) on the basic reproduction number.

Motivated by the three aspects above, we established a four-dimensional *SIR* edge-based compartmental model with two communities, and explicitly obtained the basic reproduction number $R_0(\langle l \rangle)$ with the average intercommunity degree $\langle l \rangle$. According

to $R_0(0)$ with zero intercommunity edges, a severity-based hierarchical intervention scheme of epidemics is formed. The scheme is divided into two cases. In the case 2 with $R_0(0) > 1$, epidemics break out when at least one of the reproduction number within each community is larger than one. Then, intervention measures on the inner community must be carried out to make their reproduction numbers below one. The severity in the case 2 is eased into that in the case 1. In the case 1 with $R_0(0) < 1$, epidemics may break out depending on the average intercommunity degree $\langle l \rangle$. We obtained the critical average intercommunity degree $\langle l_0 \rangle$. Below it, epidemics die out, or otherwise break out. We then applied the scheme successfully into SARS control from March 25th, 2003 to April 27th, 2003 in Singapore. The final size is acquired by proving existence of positive equilibrium of the model. Moreover, we carried out numerical simulation to verify out theoretical results in networks with degree distribution obeying Poisson distribution and Power law distribution, respectively.

The arrangement of this paper is as follows: In Sect. 2, we introduced the network with two communities and derived our model. In Sect. 3, we calculated the basic reproduction number, analyzed the relationship between the basic reproduction number and the intercommunity edges number to propose the severity-based hierarchical intervention scheme of epidemics. We then proved the existence of the final size. The results was verified by numerical simulation in Sect. 4. Finally, we draw a detailed discussion and conclusion in Sect. 5.

## 2 The edge-based compartmental model with communities

When an epidemic firstly comes, intercommunity edges are directly related to whether epidemic could be successfully contained with the minimal impacts on the locals normal life. Therefore, in the paper, we built an SIR edge-based compartmental model with communities to analyze the influence of intercommunity edges on the spread of epidemics. Next, we first introduce the network with two communities.

### 2.1 The network with two communities

As shown in Fig. 1, we consider a network of size $N$ including two communities with sizes $N_1$ and $N_2$, $N = N_1 + N_2$. Each node in the community $i$, has two types of edges: innercommunity edges (black lines) and intercommunity edges (orange lines). The size of nodes in community $i$ with $k$ innercommunity edges and $l$ intercommunity edges, is denoted by $N_i(k, l)$, $i \in \{1, 2\}$, $k = 0, \ldots, k_{max}$ ($k_{max}$ is the maximum number of innercommunity edges), $l = 0, \ldots, l_{max}$ ($l_{max}$ is the maximum number of intercommunity edges). Then, the joint degree distribution of the nodes in community $i$, $i \in \{1, 2\}$, is defined as

$$P_i(k, l) = \frac{N_i(k, l)}{N_i}, \quad k = 0, 1, \ldots, k_{max}, l = 0, 1, \ldots, l_{max}. \tag{1}$$

It represents the probability that any randomly chosen node in community $i$ has $k$ innercommunity edges and $l$ intercommunity edges. According to Eq. (1), we could give the following marginal degree distributions of the nodes in community $i$,

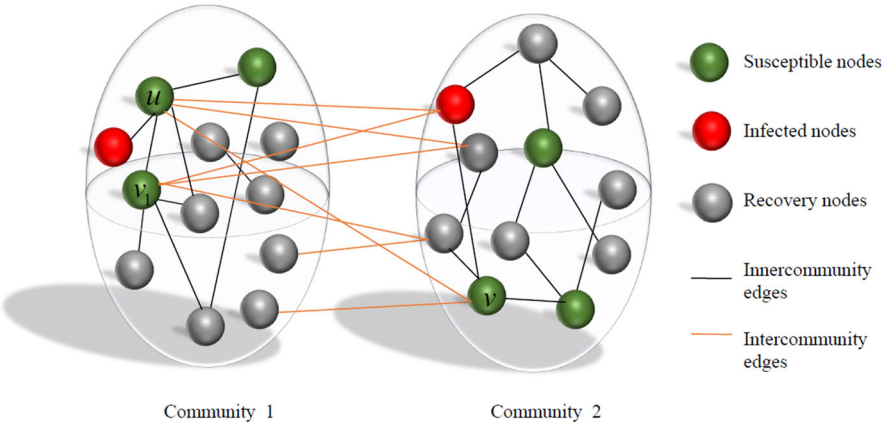


**Fig. 1** The network with two communities consists of $N$ nodes, where nodes represent individuals. Community 1 consists of $N_1$ nodes, community 2 consists of $N_2$ nodes. The black and orange lines represent innercommunity, intercommunity edges, respectively (color figure online)

$$P_{ii}(k,l) = \frac{\sum_l N_i(k,l)}{N_i} = \sum_l P_i(k,l), \quad i \in \{1,2\}, \tag{2a}$$

$$P_{ij}(k,l) = \frac{\sum_k N_i(k,l)}{N_i} = \sum_k P_i(k,l), \quad i,j \in \{1,2\}, i \neq j, \tag{2b}$$

where $k = 0,1,\ldots,k_{max}$ and $l = 0,1,\ldots,l_{max}$. In Eq. (2), $P_{ii}(k)$ represents the probability that one randomly chosen node in community $i$ has $k$ inner edges in community $i$ and $P_{ij}(l)$ represents the probability that one randomly chosen node in community $i$ has $l$ intercommunity edges.

In what follows, based on network edges, we define another type probability that one node with fixed innercommunity and intercommunity edges is reached along one randomly chosen innercommunity (or intercommunity) edge. It is also referred as the excess degree distributions of the nodes (Starnini and Pastor-Satorras 2014). Specifically, as the joint excess degree distributions will not be used in the paper, only the marginal excess degree distributions are defined as:

$$q_{ii}(k,l) = \frac{kN_i(k,l)}{\sum_k kN_i(k,l)} = \frac{kP_i(k,l)}{\sum_k kP_i(k,l)}, \quad i \in \{1,2\}, \tag{3a}$$

$$q_{ij}(k,l) = \frac{lN_i(k,l)}{\sum_l lN_i(k,l)} = \frac{lP_i(k,l)}{\sum_l lP_i(k,l)}, \quad i,j \in \{1,2\}, i \neq j. \tag{3b}$$

where $k = 0,1,\ldots,k_{max}$ and $l = 0,1,\ldots,l_{max}$. In Eq. (3), $q_{ii}(k,l)$ represents the probability that one node in community $i$ with $k$ innercommunity edges and $l$ intercommunity edges is reached along one any randomly chosen innercommunity edge in community $i$. The $q_{ij}(l)$ represents the probability that one node in community $i$ with $k$ innercommunity edges and $l$ intercommunity edges is reached along any randomly chosen intercommunity edge connected to community $j$.

Note that, in uncorrelated networks (Catanzaro et al. 2005), it has the following relations between the joint distributions in Eq. (1) and marginal distributions in Eq. (2)

$$P_i(k,l) = P_{ii}(k,l)P_{ij}(k,l), \quad i,j \in \{1,2\}, i \neq j,$$

where $k = 0, 1, \ldots, k_{max}$ and $l = 0, 1, \ldots, l_{max}$. We carried out our research in the uncorrelated networks. Our network could be generated based on the configuration model (CM) (Bender and Canfield 1978; Newman et al. 2001).

Finally, the generating functions of the above joint and marginal probabilities are respectively given as

$$\Psi_i(x,y) = \sum_{k,l} P_i(k,l)x^k y^l = \sum_{k,l} P_{ii}(k,l)P_{ij}(k,l)x^k y^l, \quad i,j \in \{1,2\}, i \neq j, \tag{4a}$$

$$\Psi_{ii}(x) = \sum_k P_{ii}(k,l)x^k, \quad \Psi_{ij}(y) = \sum_l P_{ij}(k,l)y^l, \quad i,j \in \{1,2\}, i \neq j, \tag{4b}$$

$$G_{ii}(x) = \sum_k q_{ii}(k,l)x^{k-1} = \frac{\sum_k k P_{ii}(k,l)x^{k-1}}{\langle k_{ii}\rangle}, \quad i \in \{1,2\}, k \neq 1, \tag{4c}$$

$$\tilde{G}_{ii}(x) = \sum_k q_{ii}(k,l)x^k = \frac{\sum_k k P_{ii}(k,l)x^k}{\langle k_{ii}\rangle}, \quad i \in \{1,2\}, \tag{4d}$$

$$G_{ij}(y) = \sum_l q_{ij}(k,l)y^{l-1} = \frac{\sum_l l P_{ij}(k,l)y^{l-1}}{\langle l_{ij}\rangle}, \quad i,j \in \{1,2\}, i \neq j, l \neq 1, \tag{4e}$$

$$\tilde{G}_{ij}(y) = \sum_l q_{ij}(k,l)y^l = \frac{\sum_l l P_{ij}(k,l)y^l}{\langle l_{ij}\rangle}, \quad i,j \in \{1,2\}, i \neq j, \tag{4f}$$

where $k = 0, 1, \ldots, k_{max}$ and $l = 0, 1, \ldots, l_{max}$. In Eq. (4), $\langle k_{ii}\rangle = \Psi'_{ii}(1)$ (or $\langle l_{ij}\rangle = \Psi'_{ij}(1)$) stands for the average innercommunity (or intercommunity) degrees of nodes in community $i$. The $G_{ii}(x)$ and $G_{ij}(y)$ represent the corresponding generating functions including the randomly chosen edge. The $\tilde{G}_{ii}(x)$ and $\tilde{G}_{ij}(y)$ represent corresponding generating functions excluding the randomly chosen edge. There also exists the identity relation between intercommunity edges,

$$N_1\langle l_{12}\rangle = N_2\langle l_{21}\rangle. \tag{5}$$

### 2.2 The edge-based compartmental model in a single community

In this subsection, we first briefly recall the edge-based compartmental model in a single community (Miller et al. 2012; Miller 2011), and then extend it to the edge-based compartmental model with multiple communities in next subsection. We take community 1 in the Fig. 1 as an example to start our introduction.

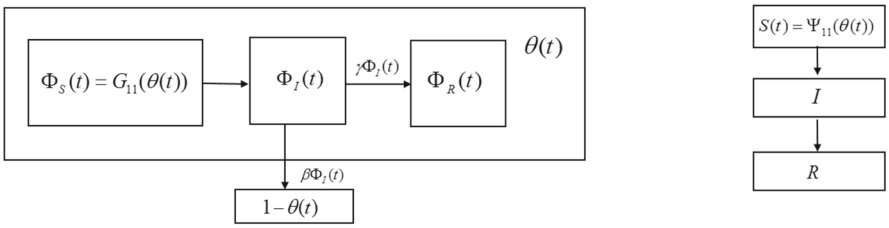


**Fig. 2** Flowchart of edge-based compartmental model (Miller et al. 2012)

In edge-based compartmental model, dynamics of nodes are characterized by dynamics of edges. For the modelling of edges, the key variable is $\theta(t)$, representing the probability that a randomly chosen edge from all edges in random graph has not transmitted infection by time $t$. It indicates that by time $t$, one end of this randomly chosen edge must be susceptible, and the other end may be one of three states: susceptible, infected and recovered. For example, the susceptible node $u$ in community 1 has neighbours of three states: susceptible $v_1$, infected $v_2$ and recovered $v_3$. In other words, it has three type edges of $S-S$, $S-I$ and $S-R$. Further, three edge-based variables $\Phi_S(t)$, $\Phi_I(t)$ and $\Phi_R(t)$ are defined, representing the probabilities that the other end of a randomly chosen edge having not transmitted infection by time $t$ is, susceptible, infected and recovered, respectively (see Fig. 2). It follows that

$$\theta(t) = \Phi_S(t) + \Phi_I(t) + \Phi_R(t). \tag{6}$$

It could be seen in Eq. (6) that change of $\theta(t)$ only depends on the change of $\Phi_I(t)$, that is, $\theta(t)$ changes only when infection occurs in $S-I$ edges. Therefore, it has

$$\dot{\theta}(t) = -\beta\Phi_I(t), \tag{7}$$

where $\beta$ is the infection rate.

For $\Phi_S(t)$, in order to ensure that the other end of a randomly chosen edge is also susceptible, the remaining edges of this end must not transmit infection to it. For example, a randomly chosen $S-S$ edge $u-v_1$, where $u$ is the susceptible node, also denoted as the test node, node $v_1$ has degree $k$, for ensuring $v_1$ is susceptible, the remaining $k-1$ edges do not transmit infection. Therefore, the probability of node $v_1$ being susceptible is $\theta^{k-1}(t)$. As diseases spread along the edges, the excess degree distribution is applied. In other words, the probability of node $v_1$ being reached along a randomly chosen edge is $\frac{kp_{11}(k)}{\langle k_{11}\rangle}$. Therefore, when $v_1$ is any node with various degrees in community 1, according to Eq. (4c), it leads to

$$\Phi_S(t) = \frac{\sum_k kP_{11}(k)\theta^{k-1}(t)}{\langle k_{11}\rangle} = \sum_k q_{11}(k)\theta^{k-1}(t) = G_{11}(\theta(t)). \tag{8}$$

For $\Phi_I$ and $\Phi_R$, when infected node recovers with rate $\gamma$, it has

$$\dot{\Phi}_R(t) = \gamma\Phi_I(t). \tag{9}$$

From Eqs. (6)–(9) with $\theta(0) = 1$ and $\Phi_R = 0$, it has

$$\Phi_I(t) = \theta(t) - \frac{\gamma}{\beta}(1 - \theta(t)) - G_{11}(\theta(t)). \tag{10}$$

Then, substituting (10) into (7) leads to an edge-based one-dimension system,

$$\dot{\theta}(t) = -\beta\theta(t) + \gamma(1 - \theta(t)) + \beta G_{11}(\theta(t)). \tag{11}$$

For the dynamics system of nodes, given a susceptible node with degree $k$, the probability that it is still susceptible by time $t$ is $\theta^k(t)$, and the probability that it is chosen randomly from all nodes is $P_{11}(k)$. It follows that the probability of any randomly chosen node being susceptible in community 1 by time $t$ is

$$S(t) = \sum_k P_{11}(k)\theta^k(t) = \Psi_{11}(\theta(t)).$$

The edge-based compartmental model in a single community could be written as:

$$\begin{aligned}
&\textit{The edge-based equation}\\
&\dot{\theta}(t) = -\beta\theta(t) + \gamma(1 - \theta(t)) + \beta G_{11}(\theta(t)),\\
&\textit{The node-based equations}\\
&\dot{R}(t) = \gamma I(t),\\
&S(t) = \sum_k p(k)\theta^k(t) = \Psi_{11}(\theta(t)),\\
&I(t) = 1 - S(t) - R(t),
\end{aligned} \tag{12}$$

where $I(t)$ or $R(t)$ represent the probability of any randomly chosen node is infected or recovered in community 1 by time $t$ respectively.

### 2.3 The edge-based compartmental model with two communities

In this subsection, we extend the system (12) in single community to system in network with two communities (see Fig. 1).

As Fig. 1 show, the network has four type edges: two type innercommunity edges and two type intercommunity edges. Therefore, we define four probabilities: $\theta_{ii}(t)$ and $\theta_{ij}(t)$, $i, j \in \{1, 2\}$. The $\theta_{ii}(t)$ represents the probability that a randomly chosen edge from all innercommunity edges in community $i$ has not transmitted infection by time $t$. $\theta_{ij}(t)$ represents the probability that a randomly chosen edge of all intercommunity edges from community $j$ to community $i$ edges has not transmitted infection by time $t$. In the following, we only derive $\theta_{11}(t)$, $\theta_{12}(t)$, so is that of $\theta_{21}(t)$ and $\theta_{22}(t)$ according to symmetry (Table 1).

Let us first derive $\theta_{11}(t)$ in community 1. Its form is similar to $\theta$ in Eq. (6) of EBCM, expressed as

$$\theta_{11}(t) = \Phi_{S:11}(t) + \Phi_{I:11}(t) + \Phi_{R:11}(t). \tag{13}$$

**Table 1** Variables and parameters in the model formulation

| Term | Meaning |
|---|---|
| $\theta_{ij}(t)$ | The probability that a randomly chosen edge from all intercommunity edges from community $j$ to community $i$ edges has not transmitted infection by time $t$, $i, j \in \{1, 2\}, i \neq j$ |
| $\beta_{ij}$ | The infection rate from infected node $j$ to susceptible node $i$, $i \in \{1, 2\}$ |
| $\gamma_i$ | The recovery rate of infected node $i$, $i \in \{1, 2\}$ |
| $\Phi_{S:ij}(t)$ | The probability that the other end of a randomly chosen edge from all intercommunity edges in community $j$ is susceptible having not transmitted infection to community $i$ by time $t$, $i, j \in \{1, 2\}, i \neq j$ |
| $\Phi_{I:ij}(t)$ | The probability that the other end of a randomly chosen edge from all intercommunity edges in community $j$ is infected having not transmitted infection to community $i$ by time $t$, $i, j \in \{1, 2\}, i \neq j$ |
| $\Phi_{R:ij}(t)$ | The probability that the other end of a randomly chosen edge from all intercommunity edges in community $j$ is recovered having not transmitted infection to community $i$ by time $t$, $i, j \in \{1, 2\}, i \neq j$ |
| $S_i(t)$ | The probability of any randomly chosen node being susceptible in community $i$ by time $t$, $i \in \{1, 2\}$ |
| $I_i(t)$ | The probability of any randomly chosen node is infected in community $i$ by time $t$, $i \in \{1, 2\}$ |
| $R_i(t)$ | The probability of any randomly chosen node is recovered in community $i$ by time $t$, $i \in \{1, 2\}$ |

In (13), $\Phi_{S:11}(t)$, $\Phi_{I:11}(t)$ and $\Phi_{R:11}(t)$ similarly represent the probabilities that the other end of a randomly chosen edge from all innercommunity edges in community 1 is susceptible, infected and recovered having not transmitted infection by time $t$.

The same form as EBCM also exists for the following equations,

$$\dot{\theta}_{11}(t) = -\beta_{11}\Phi_{I:11}(t), \tag{14}$$

$$\dot{\Phi}_{R:11}(t) = \gamma_1\Phi_{I:11}(t). \tag{15}$$

Note that $\Phi_{S:11}(t)$ is different from that in EBCM, because here a susceptible node have two types of edges: innercommunity and intercommunity edges. If one node keeps susceptible, its all type edges must not transmit infection to it. For example, when the other end node of an $S - S$ innercommunity edge in community 1 has innercommunity degree $k$ and intercommunity degree $l$, such as $v_1$ of the $S - S$ innercommunity edge $u - v_1$ in Fig. 1, the probability of keeping it susceptible by time $t$ is $\theta_{11}^{k-1}(t)\theta_{12}^{l}(t)$. In uncorrelated network, two events that one node is reached along one innercommunity edge or along one intercommunity edge are independent of each other. Therefore, the probability of node $v_1$ being reached along one randomly chosen edge of innercommunity edges or intercommunity edge is $\frac{kP_{11}(k)}{\langle k_{11}\rangle}\frac{lP_{12}(l)}{\langle l_{12}\rangle}$. It follows that

$$\Phi_{S:11}(t) = \sum_k \sum_l \frac{kP_{11}(k)}{\langle k_{11}\rangle} \frac{lP_{12}(l)}{\langle l_{12}\rangle} \theta_{11}^{k-1}(t)\theta_{12}^{l}(t)$$
$$= \left(\sum_k \frac{kP_{11}(k)}{\langle k_{11}\rangle} \theta_{11}^{k-1}(t)\right)\left(\sum_l \frac{lP_{12}(l)}{\langle l_{12}\rangle} \theta_{12}^{l}(t)\right) = G_{11}(\theta_{11}(t))\tilde{G}_{12}(\theta_{12}(t)), \tag{16}$$

where $G_{11}$ and $\tilde{G}_{12}$ are given in (4). Then, applying the same calculation as Eq. (11) in EBCM, and according to Eqs. (13)–(16) we could obtain:

$$\dot{\theta}_{11}(t) = -\beta_{11}\theta_{11}(t) + \gamma_1(1-\theta_{11}(t)) + \beta_{11}G_{11}(\theta_{11}(t))\tilde{G}_{12}(\theta_{12}(t)). \tag{17}$$

Next, let us derive $\theta_{12}(t)$. Just as $\theta_{11}(t)$, it could be expressed as,

$$\theta_{12}(t) = \Phi_{S:12}(t) + \Phi_{I:12}(t) + \Phi_{R:12}(t).$$

Similarly, $\Phi_{S:12}(t)$, $\Phi_{I:12}(t)$ and $\Phi_{R:12}(t)$ here represent the probabilities that the other end in community 2 of a randomly chosen edge from all intercommunity edges from community 2 to community 1 is susceptible, infected and recovered. Note that it should be stressed that one end of this randomly chosen edge is in community 1 and keeps susceptible. We could also easily obtain

$$\dot{\theta}_{12}(t) = -\beta_{12}\Phi_{I:12}(t),$$
$$\dot{\Phi}_{R:12}(t) = \gamma_1\Phi_{I:12}(t).$$

For $\Phi_{S:12}(t)$, different from $\Phi_{S:11}(t)$, the other end node of an $S-S$ intercommunity edge is in community 2. For example, node $v$ of the $S-S$ intercommunity edge $u-v$ in Fig. 1. has innercommunity degree $k$ and intercommunity degree $l$. Then the probability of keeping it susceptible by time $t$ is $\theta_{21}^{l-1}(t)\theta_{22}^{k}(t)$. Similarly, in uncorrelated network, the probability of node $v$ being reached along one randomly chosen edge of innercommunity edges or intercommunity edge is $\frac{lP_{21}(l)}{\langle l_{21}\rangle}\frac{kP_{22}(k)}{\langle k_{22}\rangle}$. Thus, we have,

$$\Phi_{S:12}(t) = \sum_k \sum_l \frac{lP_{21}(l)}{\langle l_{21}\rangle} \frac{kP_{22}(k)}{\langle k_{22}\rangle} \theta_{21}^{l-1}(t)\theta_{22}^{k}(t),$$
$$= \sum_l \frac{lP_{21}(l)}{\langle l_{21}\rangle} \theta_{21}^{l-1}(t) \sum_k \frac{kP_{22}(k)}{\langle k_{22}\rangle} \theta_{22}^{k}(t),$$
$$= G_{21}(\theta_{21}(t))\tilde{G}_{22}(\theta_{22}(t)),$$

where $G_{21}$ and $\tilde{G}_{22}$ are given in (4). $\theta_{12}$ could also be obtained as

$$\dot{\theta}_{12}(t) = -\beta_{12}\theta_{12}(t) + \gamma_2(1-\theta_{12}(t)) + \beta_{12}G_{21}(\theta_{21}(t))\tilde{G}_{22}(\theta_{22}(t)). \tag{18}$$

Based on the same derivation in (17) and (18), equations of $\theta_{21}(t)$ and $\theta_{22}(t)$ could be obtained. In conclusion, we obtained the edge-based four-dimension closed system:

$$\dot{\theta}_{11}(t) = -\beta_{11}\theta_{11}(t) + \gamma_1(1-\theta_{11}(t)) + \beta_{11}G_{11}(\theta_{11}(t))\tilde{G}_{12}(\theta_{12}(t)), \tag{19a}$$

$$\dot{\theta}_{12}(t) = -\beta_{12}\theta_{12}(t) + \gamma_2(1-\theta_{12}(t)) + \beta_{12}G_{21}(\theta_{21}(t))\tilde{G}_{22}(\theta_{22}(t)), \tag{19b}$$

$$\dot{\theta}_{21}(t) = -\beta_{21}\theta_{21}(t) + \gamma_1(1-\theta_{21}(t)) + \beta_{21}G_{12}(\theta_{12}(t))\tilde{G}_{11}(\theta_{11}(t)), \tag{19c}$$

$$\dot{\theta}_{22}(t) = -\beta_{22}\theta_{22}(t) + \gamma_2(1-\theta_{22}(t)) + \beta_{22}G_{22}(\theta_{22}(t))\tilde{G}_{21}(\theta_{21}(t)). \tag{19d}$$

As for the node-based equations, if a susceptible node in community $i$ has innercommunity degree $k$ and intercommunity degree $l$, the probability that it is still susceptible by time $t$ is $\theta_{ii}^k(t)\theta_{ij}^l(t)$. The probability that it is chosen randomly from all nodes is $P_{ii}(k)P_{ij}(l)$. Therefore, the probability of any randomly chosen node being susceptible in community $i$ by time $t$ is

$$\begin{aligned} S_i(t) &= \sum_{k,l} P_{ii}(k)P_{ij}(l)\theta_{ii}^k(t)\theta_{ij}^l(t) = \sum_{k,l} P_i(k,l)\theta_{ii}^k(t)\theta_{ij}^l(t) \\ &= \Psi_i(\theta_{ii}(t), \theta_{ij}(t)), \quad i,j \in \{1,2\}, i \neq j, \end{aligned}$$

where $k = 0, 1, \ldots, k_{max}$ and $l = 0, 1, \ldots, l_{max}$. Then the probability $I_i(t)$ or $R_i(t)$ of any randomly chosen node being infected or recovered in community $i$ at time $t$, could obviously obtained as

$$\begin{aligned} \dot{R}_i(t) &= \gamma_i I_i(t), \quad i \in \{1,2\}, \\ I_i(t) &= 1 - S_i(t) - R_i(t) \quad i \in \{1,2\}. \end{aligned}$$

To sum up, the edge-based compartmental model with communities couple the edge-based equations (19) with the following the node-based equations,

*The node-based equations*

$$\begin{aligned} &S_1(t) = \sum_{k,l} P_{11}(k)P_{12}(l)\theta_{11}^k(t)\theta_{12}^l(t) = \Psi_1(\theta_1(t)), \\ &\dot{R}_1(t) = \gamma_1 I_1(t), \\ &I_1(t) = 1 - S_1(t) - R_1(t), \\ &S_2(t) = \sum_{k,l} P_{22}(k)P_{21}(l)\theta_{22}^k(t)\theta_{21}^l(t) = \Psi_2(\theta_2(t)), \\ &\dot{R}_2(t) = \gamma_2 I_2(t), \\ &I_2(t) = 1 - S_2(t) - R_2(t). \end{aligned}$$

## 3 Dynamic analysis

The basic reproduction number and the final size are crucial for characterizing the severity of epidemics' spread. In this section, we firstly discuss the positivity and boundedness of solutions for system (19), and then calculate the basic reproduction number, the final size and analyze their biological implications.

### 3.1 The positivity and boundedness of solutions for system (19)

**Theorem 1** *For any initial data* $\phi = (\theta_{11}(0), \theta_{12}(0), \theta_{21}(0), \theta_{22}(0)) \in \mathbb{R}^+$, *the solutions of system (19) preserve positivity and bounded i.e, for all* $t \in \mathbb{R}$,

$$0 < \theta_{11} \leq 1, 0 < \theta_{12} \leq 1, 0 < \theta_{21} \leq 1, 0 < \theta_{22} \leq 1.$$

***Proof*** Firstly, let us prove that the right-hand side of this inequality is true, i.e, $\theta_{11} \leq 1, \theta_{12} \leq 1, \theta_{21} \leq 1, \theta_{22} \leq 1$. The conclusion is obvious from the definition of $\theta_{11}, \theta_{12}, \theta_{21}, \theta_{22}$.

Secondly, we prove that the left-hand side of this inequality is true, i.e, $\theta_{11} > 0, \theta_{12} > 0, \theta_{21} > 0, \theta_{22} > 0$. Here, reduction to absurdity is applied. For $\theta_{11}$, if $\theta_{11}(t_1) < 0$, there exists $t_2 < t_1$ such that $\theta_{11}(t_2) = 0$. From $\theta_{11}(0) > 0$, we have

$$\dot{\theta}_{11}(t_2) < 0. \tag{20}$$

In fact, it satisfies from (19a)

$$\dot{\theta}_{11}(t_2) = \gamma_1 > 0,$$

which contradicts (20). Thus, we conclude $\theta_{11}(t_1) > 0$. Similarly, $\theta_{22}(t) > 0$ could be proved.

For $\theta_{12}$, if $\theta_{12}(t_3) < 0$, there exists $t_4 < t_3$ such that

$$\theta_{12}(t_4) = 0. \tag{21}$$

From $\theta_{12}(0) > 0$, we get $\dot{\theta}_{12}(t_4) < 0$. According to (19b), it has

$$\dot{\theta}_{12}(t_4) = \gamma_2 + \beta_{12} G_{21}(\theta_{21}(t_4)) \tilde{G}_{22}(\theta_{22}(t_4)).$$

To make sure $\dot{\theta}_{12}(t_4) < 0$, $\theta_{21}(t_4) < 0$ should be satisfied. Since $\theta_{21}(0) > 0$, there exists $t_5 < t_4$ making $\theta_{21}(t_5) = 0$ and

$$\dot{\theta}_{21}(t_5) < 0. \tag{22}$$

In fact, according to (19c), we have

$$\dot{\theta}_{21}(t_5) = \gamma_1 + \beta_{21} G_{12}(\theta_{12}(t_5)) \tilde{G}_{11}(\theta_{11}(t_5)).$$

According (21), we have $\theta_{12}(t_5) > 0$, and furthermore obtain

$$\dot{\theta}_{21}(t_5) > 0,$$

which contradicts (22). Thus we conclude $\theta_{12}(t_3) > 0$. Similarly, we also can prove $\theta_{21}(t) > 0$. □

According to Theorem 1, we can define the feasible region

$$\Omega = \left\{(\theta_{11}, \theta_{12}, \theta_{21}, \theta_{22}) \in \mathbb{R}^+ : 0 < \theta_{11} \leq 1, 0 < \theta_{12} \leq 1, 0 < \theta_{21} \leq 1, 0 < \theta_{22} \leq 1\right\}.$$

### 3.2 The basic reproduction number

The basic reproduction number is the number of secondary cases one infectious case caused in a completely susceptible population. In this subsection, based on the embedded multitype branching processes (Ball and Neal 2008), we construct the next generation matrix (NGM) (Rattana et al. 2014) to calculate the basic reproduction number $R_0$. The principal eigenvalue of the NGM is the basic reproduction number. The infecting process in the early stage of an epidemic could be approximated by a branching process (Ball and Neal 2008). Here, the infecting process caused by infectious nodes in community $i$ (type-$i$ individuals) or infectious nodes community $j$ (type-$j$ individuals), $i, j \in \{1, 2\}, i \neq j$, is approximated by a two-type process. The elements of NGM are the mean number of type-$i$ individuals produced by a type-$i$ or type-$j$ individual in the branching process, $i, j \in \{1, 2\}, i \neq j$.

In details, the mean number of type-$i$ individuals produced by a type-$i$ individual, defined as the reproduction number $R_{ii}$ in community $i$, satisfies

$$R_{ii} = \frac{\beta_{ii}}{\beta_{ii} + \gamma_i} G_{ii}^{'}(1), \quad i \in \{1, 2\}, \tag{23}$$

where $G_{ii}^{'}(1)$ describes the average remaining neighbors (excess degree) except one neighbor infecting this node in community $i$ (see Eq. (4c)). Note that the reproduction number in Eq. (23) is same as that of system (12) in single community.

Since the existence of cross infections between community $i$ and community $j$, the mean number of type-$i$ individuals produced by a type-$j$ individual, defined as the reproduction number $R_{ij}$, satisfies

$$R_{ij} = \frac{\beta_{ij}}{\beta_{ij} + \gamma_j} G_{ji}^{'}(1) + \frac{\beta_{ii}}{\beta_{ii} + \gamma_i} \frac{\tilde{G}_{ii}^{'}(1) + \tilde{G}_{ij}^{'}(1) - 1}{G_{ij}^{'}(1)} \frac{\beta_{ij}}{\beta_{ij} + \gamma_j} G_{ji}^{'}(1),$$
$$i, j \in \{1, 2\}, i \neq j, \tag{24}$$

where $G_{ji}^{'}(1)$ (or $G_{ij}^{'}(1)$) describes the average remaining neighbors (excess degree) in community $j$ (or community $i$) except one neighbor infecting this node in community

$i$ (or community $j$). The $\tilde{G}'_{ii}(1)+\tilde{G}'_{ij}(1)-1$ is the average whole neighbors of nodes in community $i$ except for neighbor in community $i$ infecting this node, $i, j \in \{1,2\}$ and $i \neq j$. From the biological aspects, in Eq. (24), the first term represents the infection contribution of one infected node in community $j$ on community $i$. The second term represents the cross contribution of two communities on community $i$ as shown in bipartite network (Newman 2002). Specifically, $\frac{\beta_{ii}}{\beta_{ii}+\gamma_i}\frac{\tilde{G}'_{ii}(1)+\tilde{G}'_{ij}(1)-1}{G'_{ij}(1)}$ could be rewritten as $\frac{\beta_{ii}}{\beta_{ii}+\gamma_i}\frac{\left(\tilde{G}'_{ii}(1)+\tilde{G}'_{ij}(1)-1\right)}{G'_{ij}(1)}$, which describes the average contribution of inner infection of one infected node community $i$ on community $j$. It follows that the next generation matrix (NGM) could be given as

$$\mathrm{NGM} = \begin{pmatrix} R_{11} & R_{12} \\ R_{21} & R_{22} \end{pmatrix}.$$

Then, the basic reproduction number $R_0$, the principal eigenvalue of NGM, is

$$\begin{aligned} R_0 = {} & \frac{\beta_{11}}{\beta_{11}+\gamma_1}\frac{\beta_{12}}{\beta_{12}+\gamma_2}\frac{\beta_{21}}{\beta_{21}+\gamma_1}\frac{\beta_{22}}{\beta_{22}+\gamma_2}\left(G^{*'}_{11}(1)+G^{*'}_{12}(1)-1\right) \\ & \times\left(\tilde{G}'_{21}(1)+\tilde{G}'_{22}(1)-1\right)+\frac{\beta_{11}}{\beta_{11}+\gamma_1}\frac{\beta_{12}}{\beta_{12}+\gamma_2}\frac{\beta_{21}}{\beta_{21}+\gamma_1}G'_{21}(1) \\ & \times\left(\tilde{G}'_{11}(1)+\tilde{G}'_{12}(1)-1\right)+\frac{\beta_{12}}{\beta_{12}+\gamma_2}\frac{\beta_{21}}{\beta_{21}+\gamma_1}\frac{\beta_{22}}{\beta_{22}+\gamma_2}G'_{12}(1) \\ & \times\left(\tilde{G}'_{21}(1)+\tilde{G}'_{22}(1)-1\right)+\frac{\beta_{12}}{\beta_{12}+\gamma_2}G'_{21}(1)\frac{\beta_{21}}{\beta_{21}+\gamma_1}G'_{12}(1) \\ & +\frac{\beta_{11}}{\beta_{11}+\gamma_1}G'_{11}(1)+\frac{\beta_{22}}{\beta_{22}+\gamma_2}G'_{22}(1)-\frac{\beta_{11}}{\beta_{11}+\gamma_1}G'_{11}(1)\frac{\beta_{22}}{\beta_{22}+\gamma_2}G'_{22}(1). \end{aligned} \tag{25}$$

It also could be indirectly verified by the linearized system at the disease-free equilibrium of system (19) in the Appendix 8.

### 3.3 The final size

This subsection proves the existence of the final size of the epidemic by demonstrating the existence of positive equilibrium $E^* = (\theta^*_{11}, \theta^*_{12}, \theta^*_{21}, \theta^*_{22})$ of system (19) in domain $(0,1)^4$ based on the multitype branching process in Allen (2010).

The final size of could be expressed as the sum of the relative final size $R^*_1$ of community 1 and the relative final size $R^*_2$ of community 2, which is

$$F = gR^*_1 + (1-g)R^*_2,$$

where

$$R_1^* = 1 - \Psi_{11}(\theta_{11}^*)\Psi_{12}(\theta_{12}^*),$$
$$R_2^* = 1 - \Psi_{22}(\theta_{22}^*)\Psi_{21}(\theta_{21}^*),$$

with $g = N_1/N$ and according to Eq. (19), $\theta_{11}^*$, $\theta_{11}^*$, $\theta_{11}^*$, and $\theta_{11}^*$ satisfy,

$$\begin{aligned}
&-\beta_{11}\theta_{11}^* + \gamma_1(1-\theta_{11}^*) + \beta_{11}G_{11}(\theta_{11}^*)\tilde{G}'_{12}(\theta_{12}^*) = 0,\\
&-\beta_{12}\theta_{12}^* + \gamma_2(1-\theta_{12}^*) + \beta_{12}G_{21}(\theta_{21}^*)\tilde{G}'_{22}(\theta_{22}^*) = 0,\\
&-\beta_{21}\theta_{21}^* + \gamma_1(1-\theta_{21}^*) + \beta_{21}G_{12}(\theta_{12}^*)\tilde{G}'_{11}(\theta_{11}^*) = 0,\\
&-\beta_{22}\theta_{22}^* + \gamma_2(1-\theta_{22}^*) + \beta_{22}G_{22}(\theta_{22}^*)\tilde{G}'_{21}(\theta_{21}^*) = 0.
\end{aligned} \tag{26}$$

Considering the coupled complexity of the model (26), an explicit expression of its fixed point is hard to obtain. Therefore, we prove its existence according to Theorem 1 in the multitype branching process (Allen 2010). We give out the following theorem.

**Theorem 2** *When the condition* $\tilde{G}'_{21}(1)\tilde{G}'_{22}(1) > G'_{21}(1)G'_{22}(1)$ *holds, Eq. (19) or (26) admits a positive equilibrium* $E^* = (\theta_{11}^*, \theta_{12}^*, \theta_{21}^*, \theta_{22}^*)$ *in domain* $(0, 1)^4$.

***Proof*** Firstly, let the right sides of Eq. (19) to be zero, Eq. (26) is transformed into

$$\begin{cases}
f_1(\theta_{11}(t), \theta_{12}(t), \theta_{21}(t), \theta_{22}(t)) := \dfrac{\gamma_1 + \beta_{11}G_{11}(\theta_{11}(t))\tilde{G}_{12}(\theta_{12}(t))}{\beta_{11} + \gamma_1},\\
f_2(\theta_{11}(t), \theta_{12}(t), \theta_{21}(t), \theta_{22}(t)) := \dfrac{\gamma_2 + \beta_{12}G_{21}(\theta_{21}(t))\tilde{G}_{22}(\theta_{22}(t))}{\beta_{12} + \gamma_2},\\
f_3(\theta_{11}(t), \theta_{12}(t), \theta_{21}(t), \theta_{22}(t)) := \dfrac{\gamma_1 + \beta_{21}G_{12}(\theta_{12}(t))\tilde{G}_{11}(\theta_{11}(t))}{\beta_{21} + \gamma_1},\\
f_4(\theta_{11}(t), \theta_{12}(t), \theta_{21}(t), \theta_{22}(t)) := \dfrac{\gamma_2 + \beta_{22}G_{22}(\theta_{22}(t))\tilde{G}_{21}(\theta_{21}(t))}{\beta_{22} + \gamma_2}.
\end{cases} \tag{27}$$

According to Theorem 4.5 in Chapter 4 of Allen (2010), we also set

$$F \equiv F\left(\overline{\theta(t)}\right) = \left(f_1\left(\overline{\theta(t)}\right), \ldots, f_4\left(\overline{\theta(t)}\right)\right). \tag{28}$$

where $\theta(t) = (\theta_{11}(t), \theta_{12}(t), \theta_{21}(t), \theta_{22}(t))$ and Eq. (27) is equivalent to

$$F = \left(\overline{\theta(t)}\right).$$

Obviously, Eq. (3.3) has an equilibrium $E_0 = (1, 1, 1, 1)$ which corresponds to disease-free equilibrium of (26). The final size depends on another equilibrium of $F$ in domain $(0, 1)^4$.

According to section 4.7 in Chapter 4 of Allen (2010), we define the $4\times4$ expectation matrix,

$$\overline{M} = \left(m_{ij}\right)_{4\times4},$$

where $m_{11} = \frac{f_1\left(\overline{\theta(t)}\right)}{\theta_{11}(t)}$, $m_{12} = \frac{f_1\left(\overline{\theta(t)}\right)}{\theta_{12}(t)}$, $\ldots$ $m_{43} = \frac{f_4\left(\overline{\theta(t)}\right)}{\theta_{21}(t)}$, and $m_{44} = \frac{f_4\left(\overline{\theta(t)}\right)}{\theta_{22}(t)}$. The linear matrix $M$ of matrix $\overline{M}$ at the equilibrium $E_0 = (1, 1, 1, 1)$ is

$$M = \begin{pmatrix} \frac{\beta_{11}G'_{11}(1)}{\beta_{11}+\gamma_1} & \frac{\beta_{11}\tilde{G}'_{12}(1)}{\beta_{11}+\gamma_1} & 0 & 0 \\ 0 & 0 & \frac{\beta_{12}G'_{21}(1)}{\beta_{12}+\gamma_2} & \frac{\beta_{12}\tilde{G}'_{22}(1)}{\beta_{12}+\gamma_2} \\ \frac{\beta_{21}\tilde{G}'_{11}(1)}{\beta_{21}+\gamma_1} & \frac{\beta_{21}G'_{12}(1)}{\beta_{21}+\gamma_1} & 0 & 0 \\ 0 & 0 & \frac{\beta_{22}\tilde{G}'_{21}(1)}{\beta_{22}+\gamma_2} & \frac{\beta_{22}G'_{22}(1)}{\beta_{22}+\gamma_2} \end{pmatrix}.$$

Obviously, matrix $M$ is regular since $|M| \neq 0$. It follows that Eq. (3.3) has a fixed point in domain $(0, 1)^4$ only when the principle eigenvalue $\lambda$ of $M$ satisfy $\lambda > 1$. Next, we give the condition of $\lambda > 1$.

According to Jury criterion (Zheng et al. 2010), for the characteristic equation of a matrix, when its constant term is less than the coefficient of highest order term, the principal eigenvalue is larger than 1. The constant term of the characteristic equation of matrix $M$ is

$$c = \Big[\beta_{11}\beta_{12}\beta_{21}\beta_{22}(\tilde{G}'_{11}(1)G'_{21}(1)G'_{22}(1) + G'_{11}(1)\tilde{G}'_{21}(1)\tilde{G}'_{22}(1) - G'_{11}(1)G'_{21}(1) G'_{22}(1) - \tilde{G}'_{11}(1)\tilde{G}'_{21}(1)\tilde{G}'_{22}(1))\Big] / \left[(\beta_{11}+\gamma_1)(\beta_{12}+\gamma_2)(\beta_{21}+\gamma_1)(\beta_{22}+\gamma_2)\right].$$

Therefore, when $c > 1$, i.e., $\tilde{G}'_{21}(1)\tilde{G}'_{22}(1) > G'_{21}(1)G'_{22}(1)$, Eq. (3.3) has a fixed point $E^* = (\theta^*_{11}, \theta^*_{12}, \theta^*_{21}, \theta^*_{22})$ in domain $(0, 1)^4$. That is, when the condition $\tilde{G}'_{21}(1)\tilde{G}'_{22}(1) > G'_{21}(1)G'_{22}(1)$ holds, (26) admits a positive equilibrium $E^* = (\theta^*_{11}, \theta^*_{12}, \theta^*_{21}, \theta^*_{22})$ in domain $(0, 1)^4$. The existence of the final size is proved. □

## 4 The effect of the intercommunity edge on $R_0$

As described in Sect. 2.1, intercommunity edges play a vital role in curbing epidemics. In this section, we analyze the impact of the number of intercommunity edges on the basic reproduction number in a network with two communities. The basic reproduction number, $R_0$, is an important index for determining epidemic outbreaks. In (25), the explicit relationship between the number of intercommunity edges and $R_0$ has been presented. However, it is hard to execute theoretical analysis since $R_0$ contains four topological parameters about inter-community edges, $\Psi'_{12}(1)$, $\Psi'_{21}(1)$, $\Psi''_{12}(1)$ and $\Psi''_{21}(1)$. When the degree distribution obeys the Poisson distribution, the four parameters can be uniformly expressed by the mean of the distribution. Therefore, we

perform the analysis in the case where inter-community edges follow a Poisson distribution. We assume the node size of two communities satisfies $N_1 = N_2$. According to (4b) and (5), we have the average intercommunity degree $\langle l_{12}\rangle = \langle l_{21}\rangle \triangleq \langle l\rangle$ and $\langle l_{12}^2\rangle - \langle l_{12}\rangle = \Psi_{12}''(1) = \langle l_{21}^2\rangle - \langle l_{21}\rangle = \Psi_{21}''(1)$.

Then, the basic reproduction number $R_0$ could be simplified to the function of average intercommunity degree $\langle l\rangle$, that is

$$R_0(\langle l\rangle) = A\langle l\rangle^2 + B\langle l\rangle + C, \tag{29}$$

where

$$\begin{aligned}
A &= \frac{\beta_{12}}{\beta_{12}+\gamma_2}\frac{\beta_{21}}{\beta_{21}+\gamma_1}\left(1+\frac{\beta_{11}}{\beta_{11}+\gamma_1}+\frac{\beta_{22}}{\beta_{22}+\gamma_2}+\frac{\beta_{11}}{\beta_{11}+\gamma_1}\frac{\beta_{22}}{\beta_{22}+\gamma_2}\right),\\
B &= \frac{\beta_{12}}{\beta_{12}+\gamma_2}\frac{\beta_{21}}{\beta_{21}+\gamma_1}\left[\left(1+\frac{\beta_{22}}{\beta_{22}+\gamma_2}\right)R_{11}+\left(1+\frac{\beta_{11}}{\beta_{11}+\gamma_1}\right)R_{22}\right.\\
&\quad\left.+\frac{\beta_{11}}{\beta_{11}+\gamma_1}+\frac{\beta_{22}}{\beta_{22}+\gamma_2}+2\frac{\beta_{11}}{\beta_{11}+\gamma_1}\frac{\beta_{22}}{\beta_{22}+\gamma_2}\right],\\
C &= \frac{\beta_{12}}{\beta_{12}+\gamma_2}\frac{\beta_{21}}{\beta_{21}+\gamma_1}\left(1+\frac{\beta_{11}}{\beta_{11}+\gamma_1}+\frac{\beta_{22}}{\beta_{22}+\gamma_2}+\frac{\beta_{11}}{\beta_{11}+\gamma_1}\frac{\beta_{22}}{\beta_{22}+\gamma_2}\right)\\
&\quad+\frac{\beta_{12}}{\beta_{12}+\gamma_2}\frac{\beta_{21}}{\beta_{21}+\gamma_1}\left[\left(1+\frac{\beta_{22}}{\beta_{22}+\gamma_2}\right)(R_{11}-1)+(R_{22}-1)\right.\\
&\quad\left.\times\left(1+\frac{\beta_{11}}{\beta_{11}+\gamma_1}\right)\right]+\left(\frac{\beta_{12}}{\beta_{12}+\gamma_2}\frac{\beta_{21}}{\beta_{21}+\gamma_1}-1\right)(R_{11}-1)(R_{22}-1)+1.
\end{aligned}$$

In Eq. (29), $R_0$ is monotonically increasing with average intercommunity degree $\langle l\rangle > 0$ because of $A > 0$, $B > 0$. The result is accordant with that in Koch et al. (2013).

When $\langle l\rangle = 0$, $R_0(0) = C$. In other words, when $R_0(0) > 1$, $R_0 > 1$, epidemics break out. When $R_0(0) < 1$, it is uncertain whether $R_0 < 1$ or $R_0 > 1$, which depends on the average intercommunity degree $\langle l\rangle$. In the following, we present the results in two cases (see Table 2).

**Case 1** $R_0(0) < 1$. In the case, if $\langle l\rangle = 0$, $R_0(0) < 1$. It indicates that epidemics do not break out when two communities are completely isolated. It also means that diseases do not break out in each community under zero average intercommunity degree. That is, we consider $R_{11} < 1$ and $R_{22} < 1$. In the case, whether epidemics break out or not strongly depend on the average intercommunity degree $\langle l\rangle$.

(1) $R_{11} < 1$, $R_{22} < 1$, when $0 < \langle l\rangle < \langle l\rangle_0$, $R_0 < 1$, epidemics die out.
(2) $R_{11} < 1$, $R_{22} < 1$, when $\langle l\rangle > \langle l\rangle_0$, $R_0 > 1$, epidemics break out.

Here $\langle l\rangle > \langle l\rangle_0$ is obviously the critical threshold of average intercommunity degree. $\langle l\rangle_0$ is the number of intercommunity edges corresponding to $R_0 = 1$.

**Case 2** $R_0(0) \geq 1$. In the case, if $\langle l\rangle = 0$, $R_0(0) > 1$. It means that epidemics break out at least in one community regardless of $\langle l\rangle$.

(1) $R_{11} > 1$ and $R_{22} < 1$, or $R_{11} < 1$ and $R_{22} > 1$, $R_0 > 1$, epidemics break out.

**Table 2** Relationships between $R_{11}$,$R_{22}$ and $R_0$ about $R_0(0)$

| | Case 1 (1) $R_0(0) < 1$ | Case 1 (2) $R_0(0) < 1$ | Case 2 (1) $R_0(0) \geq 1$ | Case 2 (2) $R_0(0) \geq 1$ |
|---|---|---|---|---|
| $R_{11}$ | $< 1$ | $< 1$ | $> 1$ | $> 1$ |
| $R_{22}$ | $< 1$ | $< 1$ | $< 1$ | $> 1$ |
| $R_0$ | $< 1$ with $0 < \langle l \rangle < \langle l \rangle_0$ | $> 1$ with $\langle l \rangle > \langle l \rangle_0$ | $> 1$ | $> 1$ |

(2) $R_{11} > 1$ and $R_{22} > 1$, $R_0 > 1$, epidemics break out.

***Remark*** Cases 1 and 2 provide a severity-based hierarchical intervention scheme for epidemics. In case 2, when epidemics break out at least in one community, interventions within communities must be carried out to make the basic reproduction number in each community below 1, i.e., $R_{11} < 1$ and $R_{22} < 1$. If so, the epidemic's severity is reduced to that in case 1 from case 2. Then, epidemics could be prohibited by cutting inter-community edges, according to case 1. The intercommunity degree threshold $\langle l \rangle_0$ corresponds to the optimal intercommunity edge-cutting number that causes the least impact on the local normal life. A detailed application of SARS is presented in Sect. 5.3.

## 5 Simulations and application to the spread of SARS

In this section, we conduct simulations to verify our theoretical results and apply them to SARS control based on the reported new cases from March 25, 2003, to April 27, 2003, in Singapore (CDC 2003).

### 5.1 Degree distribution with poisson distribution

We consider two types of networks with two communities of node size $N_1 = N_2 = 1000$ and node size $N_1 = 500$, $N_2 = 1000$ in Fig. 1, respectively. Four-type edges follow the Poisson distribution, and their average degrees under case 1 and case 2 will be given in the following. The infection rate and recovery rate are set as $\beta_{11} = 0.15$, $\beta_{12} = 0.14$, $\beta_{21} = 0.17$, $\beta_{22} = 0.12$, $\gamma_1 = 0.58$, and $\gamma_2 = 0.46$, respectively. The initial conditions are set as, $S_i(0) = 0.9$, $I_i(0) = 0.1$, $R_i(0) = 0$, $i \in \{1, 2\}$ and $\theta_{11}(0) = \theta_{12}(0) = S_1(0)$, $\theta_{21}(0) = \theta_{22}(0) = S_2(0)$, respectively.

#### 5.1.1 The situation of node size $N_1 = N_2 = 1000$

Figure 3a, c present the fraction of infectious and recovered nodes under case 1 of our hierarchical intervention scheme. The average inner community degree in each community is set as 2, i.e., $\langle k_{11} \rangle = \langle k_{22} \rangle = 2$. Then, the basic reproduction number in each community has $R_{11} = R_{22} = 0.42$. The average intercommunity degree are set as 1, 3, 5, and the corresponding basic reproduction number $R_0$ is 0.82 (black), 2.25

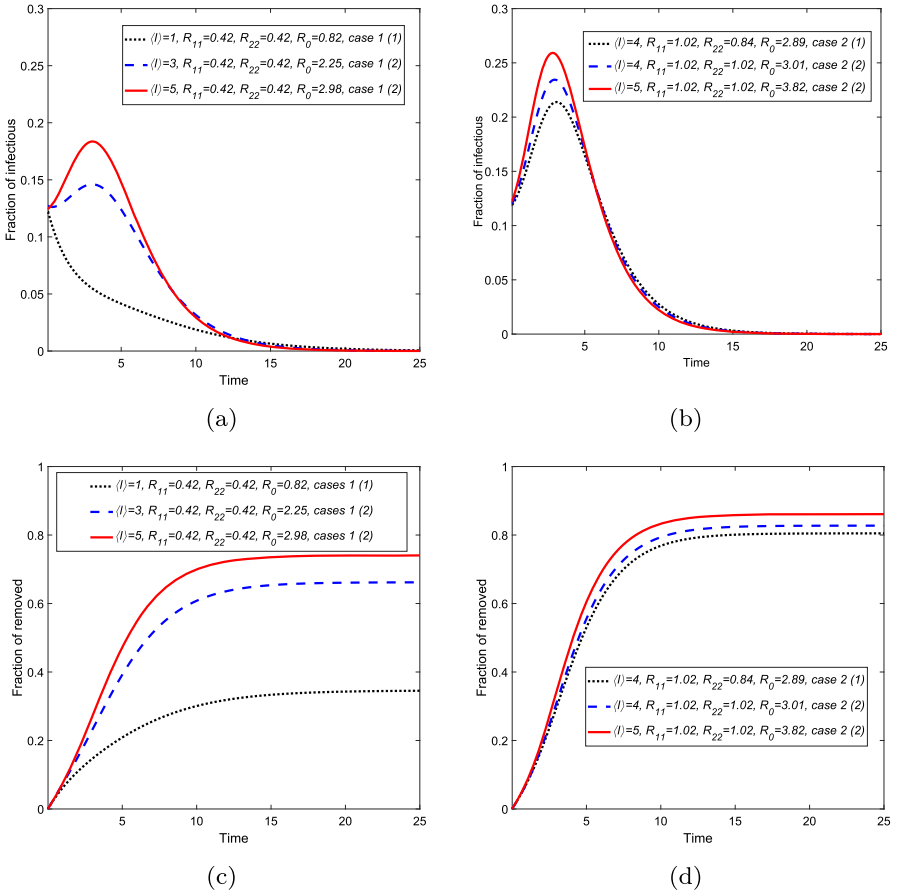


**Fig. 3** The fraction of infectious and recovered nodes under case 1 ((**a**) and (**c**)) and case 2 ((**b**) and (**d**)) for the hierarchical intervention scheme in Sect. 4

(blue) and 2.98 (red). The red and blue lines correspond to case 1 (2), and the black line corresponds to case 1 (1). It could be seen that $R_0$ decreases with the decrease of the average intercommunity degree $\langle l \rangle$. The result in case 1 suggests that epidemics could be prevented by cutting the intercommunity edges, is verified. We also see from Fig. 3c that the final size decreases with the decrease of the average intercommunity degree $\langle l \rangle$.

Figure 3b, d present the fraction of infectious and recovered nodes under case 2 of our hierarchical intervention scheme. The red and blue lines correspond to case 2 (2), with each community's average inner community degree equaling 5. The basic reproduction number in each community has $R_{11} = R_{22} = 1.02$. When the average intercommunity degree $\langle l \rangle$ declines from 5 to 4, the basic reproduction number $R_0$ decreases from 3.82 to 3.01. The infection peak and the final size also decrease. When the average inner community degree is reduced from 5 to 4 based on the blue line, but the intercommunity degree stays unchanged, the outbreak severity reduces from

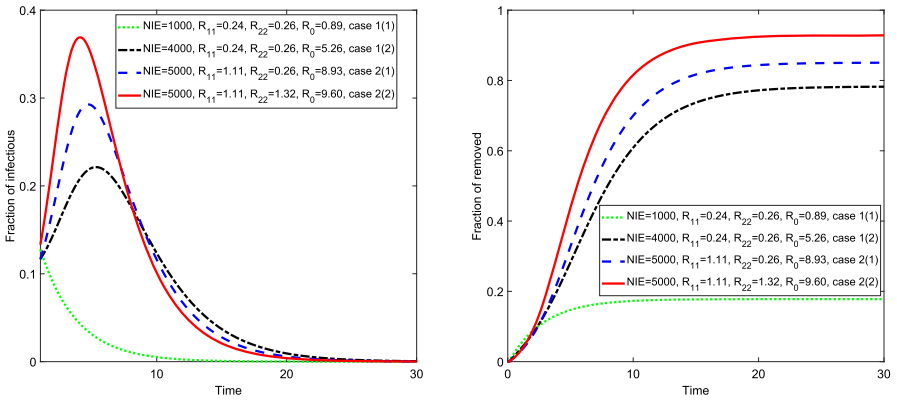


(a) (b)

**Fig. 4** The fraction of infectious and recovered nodes under case 1 (green and black) and case 2 (blue and red) for the hierarchical intervention scheme in Sect. 4 (color figure online)

case 2 (2) to case 2 (1) (black line). The result in case 2 is that reducing the basic reproduction number within a community below one could mitigate the severity of epidemics, such as by decreasing the infection peak, and the final size. That is verified.

### 5.1.2 The situation of node size $N_1 = 500$, $N_2 = 1000$

Figure 4a, b present the fraction of infectious and recovered in the hierarchical intervention scheme with node size $N_1 = 500$, $N_2 = 1000$. The average inner community degree in each community is set as 1, i.e., $\langle k_{11} \rangle = \langle k_{22} \rangle = 1$. Then, the basic reproduction number in each community has $R_{11} = 0.24$, $R_{22} = 0.26$. Note that according to Eq. (5), we here use the number of intercommunity edges ($NIE$) instead of the average intercommunity degree because the difference in node size of two communities leads to $\langle l_{12} \rangle \neq \langle l_{21} \rangle$. The $NIE$ is set at 1000, 4000, and the corresponding basic reproduction number $R_0$ is 0.89 (green) and 5.26 (black). The green line corresponds to case 1 (1), and the black line corresponds to case 1 (2). It could be seen that $R_0$ decreases with the decrease of $NIE$. The result in case 1 that cutting the intercommunity edges could curb epidemics is also verified. The blue lines correspond to case 2(1), with each community's average inner community degree equaling 4 and 1, respectively. The reproduction number in each community under case 2 (1) has $R_{11} = 1.11$, $R_{22} = 0.26$. The red lines correspond to case 2(2), with each community's average inner community degree equaling 4. The reproduction number in each community under case 2 (1) has $R_{11} = 1.11$, $R_{22} = 1.32$. When average degree in community 2 is reduced from $\langle k_{22} \rangle = 4$ to $\langle k_{22} \rangle = 1$, the basic reproduction number $R_0$ decreases from 9.60 to 8.93. The result in case 2 that reducing the inner basic reproduction number below one could mitigate the severity of epidemics is also verified.

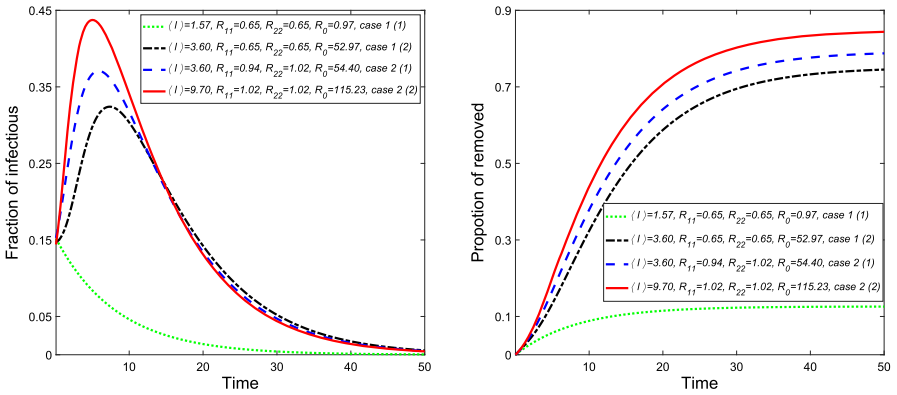


**Fig. 5** The fraction of infectious (**a**) and recovered (**b**) nodes under case 1 and case 2 for the hierarchical intervention scheme in Sect. 4

### 5.2 The degree distribution with the power law distribution

The theoretical results of our scheme are limited to the Poisson distribution of average intercommunity degrees. Here, we show the results in power law distribution. We still consider two types of network with two communities of node size $N_1 = N_2 = 1000$ and $N_1 = 500$, $N_2 = 1000$ in Fig. 1, respectively. The inner community edges follow the Poisson distribution and the intercommunity edges follow the Power law distribution.

#### 5.2.1 The situation of node size $N_1 = N_2 = 1000$

The infection rate and recovery rate are set as $\beta_{11} = 0.06, \beta_{12} = 0.07, \beta_{21} = 0.05, \beta_{22} = 0.06, \gamma_1 = 0.12$, and $\gamma_2 = 0.12$, respectively. The initial conditions are the same as in the simulation of the Poisson distribution.

Figure 5a, b present the fraction of infectious and recovered in the hierarchical intervention scheme. The average inner community degree in each community is set as 2, i.e., $\langle k_{11} \rangle = \langle k_{22} \rangle = 2$. Then, the basic reproduction number in each community has $R_{11} = R_{22} = 0.62$. The average intercommunity degree is set at 1.57, 3.60, and the corresponding basic reproduction number $R_0$ is 0.97 (green) and 52.97 (black). The green line corresponds to case 1 (1), and the black line corresponds to case 1 (2). It could also be seen that $R_0$ decreases with the decrease of the average intercommunity degree $\langle l \rangle$. The result in case 1 that cutting the intercommunity edges could curb epidemics is also verified. The red and blue lines correspond to case 2, with each community's average inner community degree equaling 2.70 and 3.03, respectively. The reproduction number in each community under case 2 (1) and case 2 (2) has $R_{11} = 0.94$, $R_{22} = 1.02$, and $R_{11} = R_{22} = 1.02$, respectively. When the average intercommunity degree $\langle l \rangle$ declines from 9.70 to 3.60, the basic reproduction number $R_0$ decreases from 115.23 to 54.40. The result in case 2 that reducing the inner reproduction number below one could mitigate the severity of epidemics is also verified.

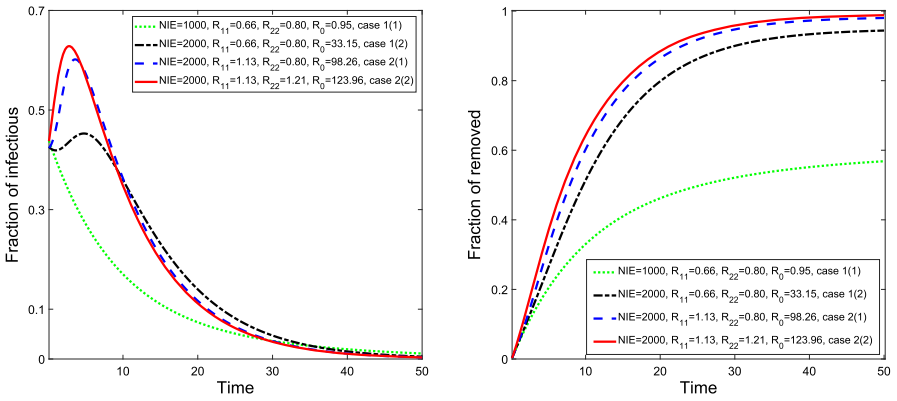


(a) (b)

**Fig. 6** The fraction of infectious and recovered nodes under case 1 (green and black) and case 2 (blue and red) for the hierarchical intervention scheme in Sect. 4 (color figure online)

### 5.2.2 The situation of node size $N_1 = 500, N_2 = 1000$

The infection rate and recovery rate are set as $\beta_{11} = 0.05, \beta_{12} = 0.04, \beta_{21} = 0.08, \beta_{22} = 0.06, \gamma_1 = 0.12$, and $\gamma_2 = 0.12$, respectively. The initial conditions are the same as in the simulation of the Poisson distribution.

Figure 6a, b present the fraction of infectious and recovered in the hierarchical intervention scheme. The average inner community degree in each community is set as 1, i.e., $\langle k_{11} \rangle = \langle k_{22} \rangle = 1$. Then, the basic reproduction number in each community has $R_{11} = 0.66$, $R_{22} = 0.80$. The $NIE$ is set at 1000, 2000, and the corresponding basic reproduction number $R_0$ is 0.95 (green) and 33.15 (black). The green line corresponds to case 1 (1), and the black line corresponds to case 1 (2). It could also be seen that $R_0$ decreases with the decrease of $NIE$. The result in case 1 that cutting the intercommunity edges could curb epidemics is also verified. The blue lines correspond to case 2(1), with each community's average inner community degree equaling 4 and 1, respectively. The reproduction number in each community under case 2 (1) has $R_{11} = 1.13, R_{22} = 0.80$. The red lines correspond to case 2(2), with each community's average inner community degree equaling 4 and 4, respectively. The reproduction number in each community under case 2 (1) has $R_{11} = 1.13$, $R_{22} = 1.21$. When average degree in community 2 is reduced from $\langle k_{22} \rangle = 2$ to $\langle k_{22} \rangle = 1$, the basic reproduction number $R_0$ decreases from 123.96 to 98.26. The result in case 2 that reducing the inner reproduction number below one could mitigate the severity of epidemics is also verified.

Although the theoretical result of the severity-based hierarchical intervention scheme for epidemics in Sect. 4 is obtained based on the equal node size of two communities and the Poisson distribution of average intercommunity degrees, it also holds when node size of two communities is different (see Fig. 4) or average intercommunity degree obeys Power law distribution (see Fig. 4). It further shows that our results have good robustness.

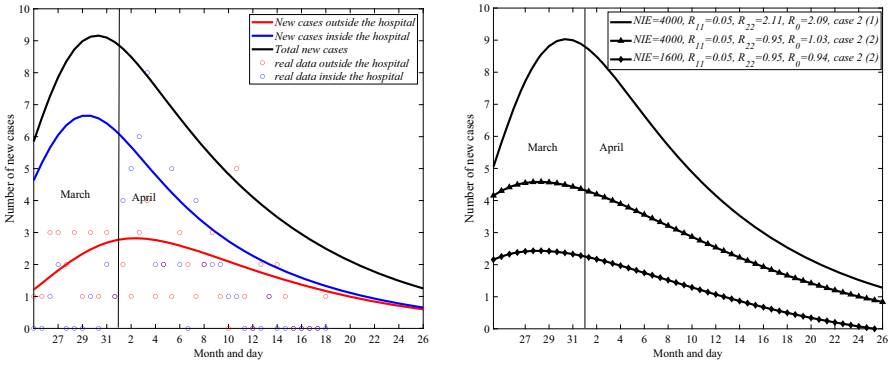


**Fig. 7** **a** Fitting model (2.1) to new cases from March 25, 2003 to April 27, 2003 in Singapore. The blue and red solid lines describe the fitted results of new cases inside and outside the hospital. The black solutions and vertical line represent the total number of new cases and the boundary between March and April. The blue and red circles represent the real data of new cases inside and outside the hospital, respectively. **b** Implementation of our hierarchical intervention scheme for SARS. The black solution line is the same as that in (**a**). The other solid-triangle and solid-rhombus lines correspond to the intervention solutions lines from case 2(1) to case 1(2), then to case 1(1) in our scheme (color figure online)

### 5.3 Applications in the transmission dynamics of SARS in Singapore

In this section, we apply the hierarchical intervention scheme in Sect. 4 to SARS based on the reported new cases from March 25, 2003, to April 27, 2003, in Singapore (CDC 2003; Magal et al. 2016). According to CDC (2003) and Magal et al. (2016), data is divided into data outside and inside the hospital (see Fig. 7a). The population size outside hospital in community 1 and inside hospital in community 2 satisfies $N_1 = 2003$ and $N_2 = 302$, respectively. As the real degree distributions are hard to obtain, we assume four types edges in network in Fig. 1 follow Poisson distributions with average degrees $\langle k_{11}\rangle = 5$, $\langle l_{12}\rangle = 2$, $\langle l_{21}\rangle = 13$ and $\langle k_{22}\rangle = 3$. Here, according to Meyers et al. (2005), considering that the average contact number in China for SARS is about eight and the basic reproduction number in China is higher than in Singapore (Meyers et al. 2005; Chowell et al. 2003), we set the average contact number outside the hospital in Singapore as $\langle k_{11}\rangle = 5$. As the protection measures in the hospital are stronger than outside the hospital (Meyers et al. 2005; Chowell et al. 2003), the average contact number inside the hospital is set as $\langle k_{22}\rangle = 3$. In CDC (2003), a superspreader could transmit ten to twenty individuals, so we set $\langle l_{21}\rangle = 13$, and naturally have $\langle l_{12}\rangle = 2$ according to Eq. (5). The initial conditions are same in CDC (2003) and Magal et al. (2016), i.e., $S_1(0) = 2000/2003$, $S_2(0) = 300$, $I_1(0) = 3/2003$, $I_2(0) = 2/302$, $R_1(0) = 0$, $R_2(0) = 0$, $\theta_{11} = 2000/2003$, $\theta_{12} = 2000/2003$, $\theta_{21} = 300/302$ and $\theta_{22} = 300/302$, respectively. Based on those, Fig. 7a present the fitted results based on the least-square method. In Fig. 7a, the vertical axis represents the number of new cases, which equals the proportion of new cases multiplied by the corresponding community node size.

In details, based on SIR epidemic transmission mechanism, we apply backward difference implicit method to obtain the number of new cases in $i$ community at time $t$ as

$$\delta_i^I(t) = (1+\gamma_i)I_i(t+1) - I_i(t), \quad i \in \{1,2\}$$

where $i = 1, 2$ represent the outside and inside of hospital. Consequently, the total number of new cases can be expressed as $\delta_1^I(t) + \delta_2^I(t)$. Correspondingly, in Fig. 7a, the red and blue solid lines describe the fitted results of new cases outside and inside the hospital. The black solution and vertical lines represent the total number of new cases and the boundary between March and April. Our fitted results are accordant with results in CDC (2003) and Magal et al. (2016). The parameters are estimated as $\beta_{11} = 0.00398, \beta_{12} = 0.00399, \beta_{21} = 0.0004$, and $\beta_{22} = 0.15, \gamma_1 = 0.04, \gamma_2 = 0.06$, respectively.

Based on the above parameters, we could obtain $R_{11} = 0.05$, $R_{22} = 2.11$ and $R_0 = 2.09$. It indicates that the scenario of the SARS outbreak in Singapore we chose corresponds to case 2 (1) of our hierarchical intervention scheme in Sect. 4. Figure 7b presents implementation effects of the hierarchical intervention scheme. The black solution line is the same as that in (a). According to our scheme, if curbing SARS, we first decrease $R_{22}$ below 1. We reduce it from 2.11 to 0.95 by decreasing the average degree $\langle k_{22} \rangle$ from 3 to 1.453. In this case, the outbreak trend is presented by a solid-triangle line in Fig. 7b, which corresponds to case 1 (2) in our scheme. Note that we here use the number of intercommunity edges (*NIE*) instead of the average intercommunity degree because the difference in node size of two communities leads to $\langle l_{12} \rangle \neq \langle l_{21} \rangle$. Further, according to our scheme, when decreasing *NIE* from 4000 to 1600, SARS dies out quickly, almost without infection peak (see the solid-rhombus line in Fig. 7b). It could be seen that SARS could be gradually contained by our hierarchical intervention scheme in Sect. 4, although the network parameters are assumed. Once the real parameters could be obtained, the results would be more accurate.

To find the important factors that affect the basic reproduction number $R_0$ and the final size, we carry out sensitivity analysis by PRCCs for all input parameters against $R_0$ (Fig. 8a) and the final size (Fig. 8b). We choose a normal distribution with 1000 samples for all parameters with $\beta_{11} = 0.00398$, $\beta_{12} = 0.00399$, $\beta_{21} = 0.0004$, $\beta_{22} = 0.15$, $\gamma_1 = 0.04$, and $\gamma_2 = 0.06$, respectively, and the respective standard deviations are $2 \times 10^{-7}$ for $\beta_{11}$, $9 \times 10^{-6}$ for $\beta_{12}$, $6 \times 10^{-7}$ for $\beta_{21}$, $6 \times 10^{-5}$ for $\beta_{22}$, $1 \times 10^{-16}$ for $\gamma_1$, and $1 \times 10^{-16}$ for $\gamma_2$. Figure 8a shows that, the transmission rate $\beta_{12}$ from infected person inside the hospital to susceptible person outside the hospital, and the transmission rate $\beta_{22}$ from infected person to susceptible person inside the hospital are the most sensitive parameters in $R_0$. It means that infected person inside the hospital have a greater impact on $R_0$. Hospitals should attach more importance to the isolation and treatment of patients inside the hospital. Figure 8b shows that, the final size is more sensitive to transmission rate $\beta_{12}$ and $\beta_{21}$ between inside hospital and outside the hospital. Thus, the government should take appropriate measures to reduce the circulating number of people inside and outside the hospital. Figure 8a, b also indicate that recovery rate $\gamma_2$ is larger than $\gamma_1$ in $R_0$ and final size. Therefore, the

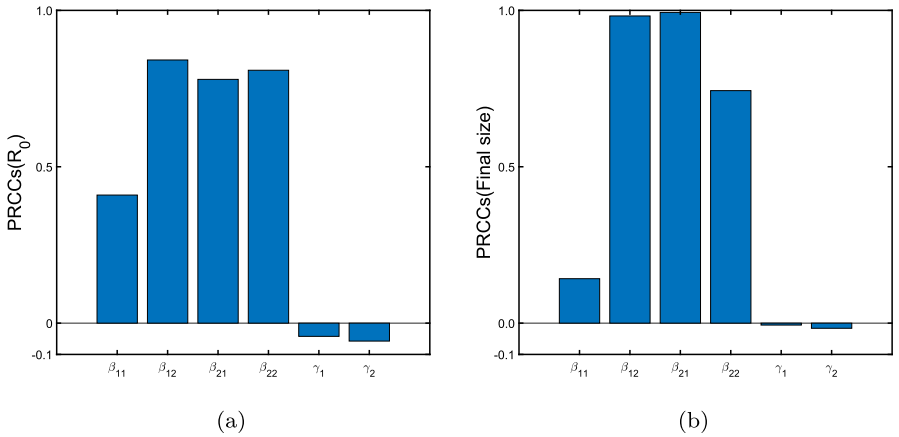


**Fig. 8** PRCCs illustrating the dependence of $R_0$ on each parameter (**a**). PRCCs illustrating the dependence of Final size on each parameter (**b**)

increase in the proportion of medical resources inside the hospital help decrease the infected risk and minimize the number of infected persons.

## 6 Discussion and conclusion

The frequent emergence of epidemics has caused a massive threat to human life, such as COVID-19 (Luo and Jin 2020; Asamoah et al. 2022). With economic globalization, the rapid spread of epidemics between communities (villages, cities, or countries) poses a significant challenge for the government to control diseases quickly. When there is no target medicine or vaccine, isolation among communities is one of the most effective intervention measures. In this case, the number of inter-community edges becomes the crucial metric measuring the degree of isolation closely related to local everyday life. Inspired by this point, we established a four-dimensional edge-based model with communities and explicitly calculated the basic reproduction number $R_0(\langle l \rangle)$ as the function of the intercommunity edges $\langle l \rangle$. We proposed a severity-based hierarchical intervention scheme for epidemics, according to $R_0(0)$ with zero inter-community edges. The scheme is divided into two cases. In case 2, $R_0(0) > 1$, epidemics break out when at least one of the inner reproduction numbers in each community is more significant than one. When the inner reproduction number is reduced to one by inner community intervention measures, the severity of case 2 is eased into that of case 1. In the case of $R_0(0) < 1$, epidemics may break out, which strongly depends on the average intercommunity degree $\langle l \rangle$. We could also obtain the critical average intercommunity degree $\langle l_0 \rangle$. In Sect. 5, we applied the scheme successfully to SARS control from March 25th, 2003, to April 27th, 2003, in Singapore. The existence of the final size is also demonstrated. Finally, to verify our theoretical results, we conducted numerical simulations in networks with degree distributions obeying the Poisson distribution and the Power law distribution.

The basic reproduction number is hard to obtain for many high-dimension edge-based models explicitly (Koch et al. 2013; Li et al. 2018; Miller and Volz 2013). We used the embedded multitype branching process method to solve the basic reproduction number from its practical significance and then verified it by disease-free stability in Sect. 8. Similarly, the final size was generally analyzed by numerical simulation for these models with more than two dimensions (Luo and Jin 2020; Koch et al. 2013; Li et al. 2018; Miller and Volz 2013). Here, we proved the existence of the final size of a four-dimensional model by using the multitype branching process and the Jury criterion. Unfortunately, the relationships between existing conditions of final size with the basic reproduction number are not found. Even so, the advances in these two aspects in the paper enhance the theoretical support for applying edge-based dynamic models to control epidemics.

The severity-based hierarchical intervention scheme of epidemics may provide a probable reference for the government to control emerging epidemics. In fact, for COVID-19, the Chinese government has made similar interventions,[1] which greatly prohibited the spread of COVID-19 in China. When one infection is confirmed in one community, the zone this community belongs to is promptly defined as the Lockdown Zone, which was put on complete lockdown. Once the intervention measures are not implemented within the zone, COVID-19 must break out. The scenario in this zone could be seen as case 2 (1) in our scheme. A control zone is defined when no new infections emerge within seven days, which could be seen as case 1 (2). If the communication between these zones is accessible, COVID-19 still breakouts. In contrast, if the communication is limited to some extent and no new infections emerge within fourteen days in the zone. This zone would be called the Precaution Zone, where COVID-19 is believed to be dying out in this zone, which could correspond to Case 1 (1).

As described above, our results mainly have the following two novelties. From the aspect of mathematics, theoretical analysis is rare for most of work on the edge-based compartmental modelling (Miller et al. 2012; Miller 2011; Rattana et al. 2014; Miller and Volz 2013; Volz 2008). In the paper, a kind of method demonstrating the positivity and boundedness of solution is provided on those models. Besides, for the high-dimension edge-based models (Rattana et al. 2014; Miller and Volz 2013), the basic reproduction number and the final size are hard to calculate and prove. We applied the embedded multitype branching process and Jury criterion to obtain the explicit basic reproduction number and demonstrate the existence of the final size of a four-dimensional model. The result provides a new insight for theoretical analysis on those edge-based compartmental models. From the aspect of application, we used a four-dimension edge-based model with community structure to explicitly give an expression of the basic reproduction number subject to *NIE*. By quantitatively analyzing their relationships, a hierarchical intervention scheme based on epidemic severity is given in Sect. 4. The critical *NIE* which could be cut off make epidemics vanish and costs minimum when an epidemic comes. Although the analyzing result is limited to the equal node size of two communities and the Poisson distribution of average intercommunity degrees, it also holds when node size of two communities is

[1] http://wjw.shanxi.gov.cn/ztzl/xxgzbdfyyqfk/jkkp/202203/t20220309_5271397.shtml.

different or average intercommunity degree obeys Power law distribution (see Fig. 4). Compared with the qualitative work about community structure (Koch et al. 2013; Li et al. 2018; Salathé and Jones 2010; Huang and Li 2007; Orman et al. 2012), our result are easier to be put into application of epidemics control, such as SARS in Singapore in Sect. 5.3.

In conclusion, we proposed a severity-based hierarchical intervention scheme for epidemics based on inter-community edges. The scheme may be used to effectively prevent the spread of epidemics, especially one newly emerging infectious disease. Unfortunately, theoretical results are limited in average intercommunity degree following Poisson distribution due to the complexity of the basic reproduction number. Modelling is limited in the uncorrelated networks because of the model complexity. In addition, we only consider cases in two communities. Epidemics break out in more communities. These could be considered in future work.

**Acknowledgements** Thank Zhenzhen Zhang, Xia Ma, Juan Zhang and Wei Zhang for their help. This research is supported by the National Natural Science Foundation of China under Grants 12101573, 12022113 and 12126416, and by Fundamental Research Program of Shanxi Province under Grants 20210302124381.

## Declarations

**Conflict of interest** The authors have no competing interests to declare that are relevant to the content of this article.

## 8 Appendix

### 8.1 Appendix A

In this subsection, we apply the linear system at disease-free equilibrium of Eq. (19) to verify the basic reproduction number in (25). The Jacobian matrix at disease-free equilibrium $E_0 = (1, 1, 1, 1)$ of model Eq. (19) is

$$\mathrm{J} = \begin{pmatrix} J_{11} & \beta_{11}\tilde{G}'_{12}(1) & 0 & 0 \\ 0 & -(\beta_{12}+\gamma_2) & \beta_{12}G'_{21}(1) & \beta_{12}\tilde{G}'_{22}(1) \\ \beta_{21}\tilde{G}'_{11}(1) & \beta_{21}G'_{12}(1) & -(\beta_{21}+\gamma_1) & 0 \\ 0 & 0 & \beta_{22}\tilde{G}'_{21}(1) & J_{44} \end{pmatrix},$$

where $J_{11} = -(\beta_{11}+\gamma_1) + \beta_{11}G'_{11}(1)$, $J_{44} = -(\beta_{22}+\gamma_2) + \beta_{22}G'_{22}(1)$.

Its characteristic equation is

$$\lambda^4 + a_1\lambda^3 + a_2\lambda^2 + a_3\lambda + a_4 = 0, \tag{30}$$

where

$$a_1 = (\beta_{11}+\gamma_1) + (\beta_{12}+\gamma_2) + (\beta_{21}+\gamma_1) + (\beta_{22}+\gamma_2) - \beta 11G'_{11}(1) - \beta_{22}G'_{22}(1),$$

$$
\begin{aligned}
a_2 &= (\beta_{11}+\gamma_1)(\beta_{12}+\gamma_2)+(\beta_{11}+\gamma_1)(\beta_{21}+\gamma_1)+(\beta_{11}+\gamma_1)(\beta_{22}+\gamma_2)\\
&\quad+(\beta_{12}+\gamma_2)(\beta_{21}+\gamma_1)+(\beta_{12}+\gamma_2)(\beta_{22}+\gamma_2)+(\beta_{21}+\gamma_1)(\beta_{22}+\gamma_2)\\
&\quad-(\beta_{12}+\gamma_2)\beta_{11}G_{11}^{'}(1)-(\beta_{21}+\gamma_1)\beta_{11}G_{11}^{'}(1-(\beta_{22}+\gamma_2)\beta_{11}G_{11}^{'}(1)\\
&\quad-(\beta_{11}+\gamma_1)\beta_{22}G_{22}^{'}(1)-(\beta_{12}+\gamma_2)\beta_{22}G_{22}^{'}(1)-(\beta_{21}+\gamma_1)\beta_{22}G_{22}^{'}(1)\\
&\quad+\beta_{11}G_{11}^{'}(1)\beta_{22}G_{22}^{'}(1)-\beta_{12}G_{21}^{'}(1)\beta_{21}G_{12}^{'}(1),\\
a_3 &= (\beta_{11}+\gamma_1)(\beta_{12}+\gamma_2)(\beta_{21}+\gamma_1)+(\beta_{11}+\gamma_1)(\beta_{12}+\gamma_2)(\beta_{22}+\gamma_2)\\
&\quad+(\beta_{11}+\gamma_1)(\beta_{21}+\gamma_1)(\beta_{22}+\gamma_2)+(\beta_{12}+\gamma_2)(\beta_{21}+\gamma_1)(\beta_{22}+\gamma_2)\\
&\quad-(\beta_{12}+\gamma_2)(\beta_{21}+\gamma_1)\beta_{11}G_{11}^{'}(1)-(\beta_{21}+\gamma_1)(\beta_{22}+\gamma_2)\beta_{11}G_{11}^{'}(1)\\
&\quad-(\beta_{12}+\gamma_2)G_{22}^{'}(1)\beta_{11}G_{11}^{'}(1)-(\beta_{11}+\gamma_1)(\beta_{21}+\gamma_1)\beta_{22}G_{22}^{'}(1)\\
&\quad-(\beta_{11}+\gamma_1)(\beta_{12}+\gamma_2)\beta_{22}G_{22}^{'}(1)-(\beta_{12}+\gamma_2)(\beta_{21}+\gamma_1)\beta_{22}G_{22}^{'}(1)\\
&\quad-(\beta_{11}+\gamma_1)\beta_{12}G_{21}^{'}(1)\beta_{21}G_{12}^{'}(1)-(\beta_{22}+\gamma_2)\beta_{12}G_{21}^{'}(1)\beta_{21}G_{12}^{'}(1)\\
&\quad+(\beta_{12}+\gamma_2)\beta_{11}G_{11}^{'}(1)\beta_{22}G_{22}^{'}(1)+(\beta_{21}+\gamma_1)\beta_{11}G_{11}^{'}(1)\beta_{22}G_{22}^{'}(1)\\
&\quad+\beta_{11}G_{11}^{'}(1)\beta_{12}G_{21}^{'}(1)\beta_{21}G_{12}^{'}(1)+\beta_{12}G_{21}^{'}(1)\beta_{21}G_{12}^{'}(1)\beta_{22}G_{22}^{'}(1)\\
&\quad-\beta_{11}\tilde{G}_{11}^{'}(1)\beta_{21}\tilde{G}_{12}^{'}(1)\beta_{12}G_{21}^{'}(1)-\beta_{12}\tilde{G}_{21}^{'}(1)\beta_{22}\tilde{G}_{22}^{'}(1)\beta_{21}G_{12}^{'}(1),\\
a_4 &= (\beta_{11}+\gamma_1)(\beta_{12}+\gamma_2)(\beta_{21}+\gamma_1)(\beta_{22}+\gamma_2)-(\beta_{12}+\gamma_2)(\beta_{21}+\gamma_1)\\
&\quad\times(\beta_{22}+\gamma_2)\beta_{11}G_{11}^{'}(1)-(\beta_{11}+\gamma_1)(\beta_{12}+\gamma_2)(\beta_{21}+\gamma_1)\beta_{22}G_{22}^{'}(1)\\
&\quad+(\beta_{22}+\gamma_2)\beta_{11}G_{11}^{'}(1)\beta_{12}G_{21}^{'}(1)\beta_{21}G_{12}^{'}(1)+(\beta_{11}+\gamma_1)\beta_{22}G_{22}^{'}(1)\\
&\quad\times\beta_{12}G_{21}^{'}(1)\beta_{21}G_{12}^{'}(1)-(\beta_{11}+\gamma_1)(\beta_{22}+\gamma_2)\beta_{12}G_{21}^{'}(1)\beta_{21}G_{12}^{'}(1)\\
&\quad+(\beta_{12}+\gamma_2)(\beta_{21}+\gamma_1)\beta_{11}G_{11}^{'}(1)\beta_{22}G_{22}^{'}(1)-(\beta_{22}+\gamma_2)\beta_{11}\tilde{G}_{11}^{'}(1)\\
&\quad\times\beta_{21}\tilde{G}_{12}^{'}(1)\beta_{12}G_{21}^{'}(1)-(\beta_{11}+\gamma_1)\beta_{12}\tilde{G}_{21}^{'}(1)\beta_{22}\tilde{G}_{22}^{'}(1)\beta_{21}G_{12}^{'}(1)\\
&\quad+\beta_{11}\tilde{G}_{11}^{'}(1)\beta_{21}\tilde{G}_{12}^{'}(1)\beta_{12}G_{21}^{'}(1)\beta_{22}G_{22}^{'}(1)+\beta_{12}\tilde{G}_{21}^{'}(1)\beta_{22}\tilde{G}_{22}^{'}(1)\\
&\quad\times\beta_{11}G_{11}^{'}(1)\beta_{21}G_{12}^{'}(1)-\beta_{11}G_{11}^{'}(1)\beta_{12}G_{21}^{'}(1)\beta_{21}G_{12}^{'}(1)\beta_{22}G_{22}^{'}(1)\\
&\quad-\beta_{11}G_{11}^{*'}(1)\beta_{12}\tilde{G}_{21}^{'}(1)\beta_{21}\tilde{G}_{12}^{'}(1)\beta_{22}\tilde{G}_{22}^{'}(1).
\end{aligned}
$$

As the complexity of the fourth order Eq. (30), the stability of disease-free equilibrium is hard to verify by Routh–Hurwitz criterion. However, for the type of edge-based equations, reference Rattana et al. (2014) has indicated that the case of $a_4 = 0$ in fourth order equation (30) is equivalent to $R_0 = 1$. Therefore, when $a_4 = 0$ in (30), we obtain

$$
\begin{aligned}
R_0 &= \frac{\beta_{11}}{\beta_{11}+\gamma_1}\frac{\beta_{12}}{\beta_{12}+\gamma_2}\frac{\beta_{21}}{\beta_{21}+\gamma_1}\frac{\beta_{22}}{\beta_{22}+\gamma_2}\left(\tilde{G}_{11}^{'}(1)+\tilde{G}_{12}^{'}(1)-1\right)\\
&\quad\times\left(\tilde{G}_{21}^{'}(1)+\tilde{G}_{22}^{'}(1)-1\right)+\frac{\beta_{11}}{\beta_{11}+\gamma_1}\frac{\beta_{12}}{\beta_{12}+\gamma_2}\frac{\beta_{21}}{\beta_{21}+\gamma_1}G_{21}^{'}(1)\\
&\quad\times\left(\tilde{G}_{11}^{'}(1)+\tilde{G}_{12}^{'}(1)-1\right)+\frac{\beta_{12}}{\beta_{12}+\gamma_2}\frac{\beta_{21}}{\beta_{21}+\gamma_1}\frac{\beta_{22}}{\beta_{22}+\gamma_2}G_{12}^{'}(1)
\end{aligned}
$$

$$\times \left(\tilde{G}'_{21}(1) + \tilde{G}'_{22}(1) - 1\right) + \frac{\beta_{12}}{\beta_{12}+\gamma_2} G'_{21}(1) \frac{\beta_{21}}{\beta_{21}+\gamma_1} G'_{12}(1)$$
$$+ \frac{\beta_{11}}{\beta_{11}+\gamma_1} G'_{11}(1) + \frac{\beta_{22}}{\beta_{22}+\gamma_2} G'_{22}(1) - \frac{\beta_{11}}{\beta_{11}+\gamma_1} G'_{11}(1) \frac{\beta_{22}}{\beta_{22}+\gamma_2} G'_{22}(1).$$

It indirectly verifies the validity of $R_0$ in (25), although the analysis lacks strict proof.

## References


Allen L (2010) An introduction to stochastic processes with applications to biology, 2nd edn. Chapman and Hall/CRC. https://doi.org/10.1201/b12537

Arino J, Bajeux N, Kirkland S (2019) Number of source patches required for population persistence in a source-sink metapopulation with explicit movement. Bull Math Biol 81:1916. https://doi.org/10.1007/s11538-019-00593-1

Arino J, Boëlle PY, Milliken E, Portet S (2021) Risk of COVID-19 variant importation? How useful are travel control measures? Infect Dis Model 6:875. https://doi.org/10.1016/j.idm.2021.06.006

Asamoah JKK, Okyere E, Abidemi A, Moore SE, Sun GQ, Jin Z, Acheampong E, Gordon JF (2022) Optimal control and comprehensive cost-effectiveness analysis for COVID-19. Results Phys 33:105177. https://doi.org/10.1016/j.rinp.2022.105177

Bajiya VP, Tripathi JP, Kakkar V, Wang J, Sun G (2021) Global dynamics of a multi-group SEIR epidemic model with infection age. Chin Ann Math Ser B 42(6):833. https://doi.org/10.1007/s11401-021-0294-1

Ball F, Neal P (2008) Network epidemic models with two levels of mixing. Math Biosci 212(1):69. https://doi.org/10.1016/j.mbs.2008.01.001

Bavel JJV, Baicker K, Boggio PS, Capraro V, Cichocka A, Cikara M, Crockett MJ, Crum AJ, Douglas KM, Druckman JN et al (2020) Using social and behavioural science to support COVID-19 pandemic response. Nat Hum Behav 4(5):460. https://doi.org/10.1038/s41562-020-0884-z

Bender EA, Canfield ER (1978) The asymptotic number of labeled graphs with given degree sequences. J Combin Theory Ser A 24(3):296. https://doi.org/10.1016/0097-3165(78)90059-6

Boily MC, Lowndes C, Alary M (2002) The impact of HIV epidemic phases on the effectiveness of core group interventions: insights from mathematical models. Sex Transm Infect 78(suppl 1):i78. https://doi.org/10.1136/sti.78.suppl_1.i78

Buonomo B, Lacitignola D, de León CV (2014) Qualitative analysis and optimal control of an epidemic model with vaccination and treatment. Math Comput Simul 100:88. https://doi.org/10.1016/j.matcom.2013.11.005

Butler D (2014) Ebola experts seek to expand testing. Nature 516(7530):154. https://doi.org/10.1038/516154a

C for Disease Control P (CDC) (2003) Severe acute respiratory syndrome? Singapore. MMWR Morb Mortal Wkly Rep 52:405

Cao X (2020) COVID-19: immunopathology and its implications for therapy. Nat Rev Immunol 20(5):269. https://doi.org/10.1038/s41577-020-0308-3

Catanzaro M, Boguná M, Pastor-Satorras R (2005) Generation of uncorrelated random scale-free networks. Phys Rev E 71(2):027103. https://doi.org/10.1103/PhysRevE.71.027103

Chen L, Sun J (2014) Global stability and optimal control of an SIRS epidemic model on heterogeneous networks. Phys A Stat Mech Appl 410:196. https://doi.org/10.1016/j.physa.2014.05.034

Chen L, Sun J (2014) Optimal vaccination and treatment of an epidemic network model. Phys Lett A 378:3028. https://doi.org/10.1016/j.physleta.2014.09.002

Chowdhury R, Heng K, Shawon M, Goh G, Franco OH (2020) Dynamic interventions to control COVID-19 pandemic: a multivariate prediction modelling study comparing 16 worldwide countries. Eur J Epidemiol 35(1):1. https://doi.org/10.1007/s10654-020-00649-w

Chowell G, Fenimore P, Castillo-Garsow M, Castillo-Chavez C (2003) SARS outbreaks in Ontario, Hong Kong and Singapore: the role of diagnosis and isolation as a control mechanism. J Theor Biol 224(1):1. https://doi.org/10.1016/S0022-5193(03)00228-5

Clara S, Remco VDH, Johan SHVL (2016) Epidemic spreading on complex networks with community structures. Sci Rep 6(1):1. https://doi.org/10.1038/srep29748
de Jesus Esquivel-Gómez J, Barajas-Ramírez JG (2018) Efficiency of quarantine and self-protection processes in epidemic spreading control on scale-free networks. Chaos 28(1):013119. https://doi.org/10.1063/1.5001176
Feng S, Luo X, Pei X, Jin Z, Lewis M, Wang H (2022) Modeling the early transmission of COVID-19 in New York and San Francisco using a pairwise network model. Infect Dis Model 7(1):19. https://doi.org/10.1016/j.idm.2021.12.009
Forster GA, Gilligan CA (2007) Optimizing the control of disease infestations at the landscape scale. Proc Natl Acad Sci 104:4984. https://doi.org/10.1073/pnas.0607900104
Fraser C, Riley S, Anderson RM, Ferguson NM (2004) Factors that make an infectious disease outbreak controllable. Proc Natl Acad Sci 101(16):6146. https://doi.org/10.1073/PNAS.0307506101
Fu X, Small M, Walker DM, Zhang H (2008) Epidemic dynamics on scale-free networks with piecewise linear infectivity and immunization. Phys Rev E 77:036113. https://doi.org/10.1103/PhysRevE.77.036113
Guo J, Huang F, Liu J, Chen Y, Wang W, Cao B, Zou Z, Liu S, Pan J, Bao C et al (2015) The serum profile of hypercytokinemia factors identified in H7N9-infected patients can predict fatal outcomes. Sci Rep 5(1):1. https://doi.org/10.1038/srep21230
Halloran ME, Jr I, Nizam A, Yang Y (2002) Containing bioterrorist smallpox. Science 298(5597):1428. https://doi.org/10.1126/science.1074674
Hammarlund E, Lewis MW, Hansen SG, Strelow LI, Nelson JA, Sexton GJ, Hanifin JM, Slifka MK (2003) Duration of antiviral immunity after smallpox vaccination. Nat Med 9:1131. https://doi.org/10.1038/nm917
Haynes BF, Pantaleo G, Fauci AS (1996) Toward an understading of the correlates of protective immunity to HIV infection. Science 271(5247):324. https://doi.org/10.1126/science.271.5247.324
Horby P (2013) H7N9 is a virus worth worrying about. Nature 496(7446):399. https://doi.org/10.1038/496399a
Huang W, Li C (2007) Epidemic spreading in scale-free networks with community structure. J Stat Mech Theory Exp 2007(01):P01014. https://doi.org/10.1088/1742-5468/2007/01/P01014
Huang W, Li C (2007) Epidemic spreading in scale-free networks with community structure. J Stat Mech Theory Exp 2007:P01014. https://doi.org/10.1088/1742-5468/2007/01/P01014
Iacoviello D, Stasio N (2013) Optimal control for SIRC epidemic outbreak. Comput Methods Programs Biomed 110:333. https://doi.org/10.1016/j.cmpb.2013.01.006
Jin EM, Girvan M, Newman M (2001) The structure of growing social networks. Work Pap 64(4 Pt 2):046132. https://doi.org/10.1103/PhysRevE.64.046132
Jin Z, Zhang J, Song LP, Sun GQ, Kan J, Zhu H (2011) Modelling and analysis of influenza A (H1N1) on networks. BMC Public Health 11(1):1. https://doi.org/10.1186/1471-2458-11-S1-S9
Kandhway K, Kuri J (2014) How to run a campaign: optimal control of SIS and SIR information epidemics. Appl Math Comput 231:79. https://doi.org/10.1016/j.amc.2013.12.164
Kandhway K, Kuri J (2014) Optimal control of information epidemics modeled as Maki Thompson rumors. Commun Nonlinear Sci Numer Simul 19(12):4135. https://doi.org/10.1016/j.cnsns.2014.04.022
Kang H, Liu K, Fu X (2017) Dynamics of an epidemic model with quarantine on scale-free networks. Phys Lett A 381(47):3945. https://doi.org/10.1016/j.physleta.2017.09.040
Keeling MJ, Gilligan CA (2000) Metapopulation dynamics of bubonic plague. Nature 407(6806):903. https://doi.org/10.1038/35038073
Koch D, Illner R, Ma J (2013) Edge removal in random contact networks and the basic reproduction number. J Math Biol 67(2):217. https://doi.org/10.1007/s00285-012-0545-6
Kostyuchenko VA, Lim EXY, Zhang S, Fibriansah G, Ng TS, Ooi JSG, Shi J, Lok SM (2016) Structure of the thermally stable Zika virus. Nature 533(7603):425. https://doi.org/10.1038/nature17994
Larocca RA, Abbink P, Peron JPS, de Zanotto PM, Iampietro MJ, Badamchi-Zadeh A, Boyd M, Ng'ang'a D, Kirilova M, Nityanandam R et al (2016) Vaccine protection against Zika virus from Brazil. Nature 536(7617):474. https://doi.org/10.1038/nature18952
Li J, Wang J, Jin Z (2018) SIR dynamics in random networks with communities. J Math Biol 77(4):1117. https://doi.org/10.1007/s00285-018-1247-5
Liu Z, Hu B (2005) Epidemic spreading in community networks. Europhys Lett 72(2):315. https://doi.org/10.1209/epl/i2004-10550-5

Lloyd-Smith JO, George D, Pepin KM, Pitzer VE, Pulliam J, Dobson AP, Hudson PJ, Grenfell BT (2009) Epidemic dynamics at the human–animal interface. Science 326:1362. https://doi.org/10.1126/science.1177345
Lu L, Jia M, Ma Y, Yang L, Chen Z, Ho DD, Jiang Y, Zhang L (2008) The changing face of HIV in China. Nature 455(7213):609. https://doi.org/10.1038/455609a
Luo X, Jin Z (2020) A new insight into isolating the high-degree nodes in network to control infectious diseases. Commun Nonlinear Sci Numer Simul 91:105363. https://doi.org/10.1016/j.cnsns.2020.105363
Ma X, Luo XF, Li L, Li Y, Sun GQ (2022) The influence of mask use on the spread of COVID-19 during pandemic in New York City. Results Phys 34:105224. https://doi.org/10.1016/j.rinp.2022.105224
Madar N, Kalisky T, Cohen R, ben Avraham D, Havlin S (2004) Immunization and epidemic dynamics in complex networks. Eur Phys J B 38:269. https://doi.org/10.1140/epjb/e2004-00119-8
Magal P, Seydi O, Webb G (2016) Final size of an epidemic for a two-group SIR model. SIAM J Appl Math 76(5):2042. https://doi.org/10.1137/16M1065392
Meyers LA, Pourbohloul B, Newman M, Skowronski DM, Brunham RC (2005) Network theory and SARS: predicting outbreak diversity. J Theor Biol 232(1):71. https://doi.org/10.1016/j.jtbi.2004.07.026
Miller JC (2011) A note on a paper by Erik Volz: SIR dynamics in random networks. J Math Biol 62(3):349. https://doi.org/10.1007/s00285-010-0337-9
Miller JC, Volz EM (2013) Incorporating disease and population structure into models of SIR disease in contact networks. PLoS ONE 8(8):e69162. https://doi.org/10.1371/journal.pone.0069162
Miller JC, Slim AC, Volz EM (2012) Edge-based compartmental modelling for infectious disease spread. J R Soc Interface 9(70):890. https://doi.org/10.1098/rsif.2011.0403
Momoh AA, Fügenschuh A (2018) Optimal control of intervention strategies and cost effectiveness analysis for a Zika virus model. Oper Res Health Care 18:99. https://doi.org/10.1016/j.orhc.2017.08.004
Mt V, Bickmann J, Wittkowski R (2020) Effects of social distancing and isolation on epidemic spreading: a dynamical density functional theory model. arXiv preprint arXiv:2003.13967
Newman M (2002) The spread of epidemic disease on networks. Phys Rev E Stat Nonlinear Soft Matter Phys 66(1 Pt 2):016128. https://doi.org/10.1103/PhysRevE.66.016128
Newman ME, Strogatz SH, Watts DJ (2001) Random graphs with arbitrary degree distributions and their applications. Phys Rev E 64(2):026118. https://doi.org/10.1103/PhysRevE.64.026118
Nowzari C, Preciado VM, Pappas GJ (2016) Analysis and control of epidemics: a survey of spreading processes on complex networks. IEEE Control Syst Mag 36(1):26. https://doi.org/10.1109/MCS.2015.2495000
Orman GK, Labatut V, Cherifi H (2012) An empirical study of the relation between community structure and transitivity. Workshop Complex Netw. https://doi.org/10.1007/978-3-642-30287-9_11
Pandey A, Atkins KE, Medlock J, Wenzel N, Townsend JP, Childs JE, Nyenswah TG, Ndeffo-Mbah ML, Galvani AP (2014) Strategies for containing Ebola in West Africa. Science 346(6212):991. https://doi.org/10.1126/science.1260612
Pastor-Satorras R, Vespignani A (2002) Immunization of complex networks. Phys Rev E 65:036104. https://doi.org/10.1103/PhysRevE.65.036104
Peng L, Yang W, Zhang D, Zhuge C, Hong L (2020) Epidemic analysis of COVID-19 in China by dynamical modeling. arXiv preprint arXiv:2002.06563
Rattana P, Miller JC, Kiss IZ (2014) Pairwise and edge-based models of epidemic dynamics on correlated weighted networks. Math Model Nat Phenom 9(2):58. https://doi.org/10.1051/mmnp/20149204
Rowthorn RE, Laxminarayan R, Gilligan CA (2009) Optimal control of epidemics in metapopulations. J R Soc Interface. https://doi.org/10.1098/rsif.2008.0402
Salathé M, Jones JH (2010) Dynamics and control of diseases in networks with community structure. PLoS Comput Biol. https://doi.org/10.1371/journal.pcbi.1000736
Salathé M, Jones JH (2010) Dynamics and control of diseases in networks with community structure. PLoS Comput Biol 6(4):e1000736. https://doi.org/10.1371/journal.pcbi.1000736
Singh RK, Dhama K, Khandia R, Munjal A, Karthik K, Tiwari R, Chakraborty S, Malik YS, Bueno-Marí R (2018) Prevention and control strategies to counter Zika virus, a special focus on intervention approaches against vector mosquitoes current updates. Front Microbiol 9:87. https://doi.org/10.3389/fmicb.2018.00087
Starnini M, Pastor-Satorras R (2014) Temporal percolation in activity-driven networks. Phys Rev E 89(3):032807. https://doi.org/10.1103/PhysRevE.89.032807
Strona G, Castellano C (2018) Rapid decay in the relative efficiency of quarantine to halt epidemics in networks. Phys Rev E 97:022308. https://doi.org/10.1103/PhysRevE.97.022308

Volz E (2008) SIR dynamics in random networks with heterogeneous connectivity. J Math Biol 56(3):293. https://doi.org/10.1007/s00285-007-0116-4
Xu Z, Li K, Sun M, Fu X (2019) Interaction between epidemic spread and collective behavior in scale-free networks with community structure. J Theor Biol 462:122. https://doi.org/10.1016/j.jtbi.2018.11.003
Yan X, Zou Y (2008) Optimal and sub-optimal quarantine and isolation control in SARS epidemics. Math Comput Model 47(1):235. https://doi.org/10.1016/j.mcm.2007.04.003
Yuan P, Tan Y, Yang L, Aruffo E, Ogden NH, Belair J, Arino J, Heffernan JM, Watmough J, Carabin H et al (2022) Modelling vaccination and control strategies of outbreaks of monkeypox at gatherings. Front Public Health. https://doi.org/10.3389/fpubh.2022.1026489
Zheng B, Liang L, Zhang C (2010) Extended jury criterion. Science China Math 53(4):1133. https://doi.org/10.1007/s11425-009-0208-2
Zuzek LG, Stanley HE, Braunstein LA (2015) Epidemic model with isolation in multilayer networks. Sci Rep 5(1):1. https://doi.org/10.1038/srep12151

# Terms and Conditions

Springer Nature journal content, brought to you courtesy of Springer Nature Customer Service Center GmbH ("Springer Nature").

Springer Nature supports a reasonable amount of sharing of research papers by authors, subscribers and authorised users ("Users"), for small-scale personal, non-commercial use provided that all copyright, trade and service marks and other proprietary notices are maintained. By accessing, sharing, receiving or otherwise using the Springer Nature journal content you agree to these terms of use ("Terms"). For these purposes, Springer Nature considers academic use (by researchers and students) to be non-commercial.

These Terms are supplementary and will apply in addition to any applicable website terms and conditions, a relevant site licence or a personal subscription. These Terms will prevail over any conflict or ambiguity with regards to the relevant terms, a site licence or a personal subscription (to the extent of the conflict or ambiguity only). For Creative Commons-licensed articles, the terms of the Creative Commons license used will apply.

We collect and use personal data to provide access to the Springer Nature journal content. We may also use these personal data internally within ResearchGate and Springer Nature and as agreed share it, in an anonymised way, for purposes of tracking, analysis and reporting. We will not otherwise disclose your personal data outside the ResearchGate or the Springer Nature group of companies unless we have your permission as detailed in the Privacy Policy.

While Users may use the Springer Nature journal content for small scale, personal non-commercial use, it is important to note that Users may not:

1. use such content for the purpose of providing other users with access on a regular or large scale basis or as a means to circumvent access control;
2. use such content where to do so would be considered a criminal or statutory offence in any jurisdiction, or gives rise to civil liability, or is otherwise unlawful;
3. falsely or misleadingly imply or suggest endorsement, approval , sponsorship, or association unless explicitly agreed to by Springer Nature in writing;
4. use bots or other automated methods to access the content or redirect messages
5. override any security feature or exclusionary protocol; or
6. share the content in order to create substitute for Springer Nature products or services or a systematic database of Springer Nature journal content.

In line with the restriction against commercial use, Springer Nature does not permit the creation of a product or service that creates revenue, royalties, rent or income from our content or its inclusion as part of a paid for service or for other commercial gain. Springer Nature journal content cannot be used for inter-library loans and librarians may not upload Springer Nature journal content on a large scale into their, or any other, institutional repository.

These terms of use are reviewed regularly and may be amended at any time. Springer Nature is not obligated to publish any information or content on this website and may remove it or features or functionality at our sole discretion, at any time with or without notice. Springer Nature may revoke this licence to you at any time and remove access to any copies of the Springer Nature journal content which have been saved.

To the fullest extent permitted by law, Springer Nature makes no warranties, representations or guarantees to Users, either express or implied with respect to the Springer nature journal content and all parties disclaim and waive any implied warranties or warranties imposed by law, including merchantability or fitness for any particular purpose.

Please note that these rights do not automatically extend to content, data or other material published by Springer Nature that may be licensed from third parties.

If you would like to use or distribute our Springer Nature journal content to a wider audience or on a regular basis or in any other manner not expressly permitted by these Terms, please contact Springer Nature at

onlineservice@springernature.com